Article published online: 2022-02-07

Tea Tree Oil and Terpinen-4-Ol Induce Cytoskeletal Reorganization of Human Melanoma Cells

OPEN ACCESS

Authors
Giuseppina Bozzuto[1], Fulvia Mariano[1], Ilaria Costa[2], Annarica Calcabrini[1], Agnese Molinari[1]

Affiliations
1 Centro Nazionale per la Ricerca e la Valutazione preclinica e clinica dei Farmaci, Istituto Superiore di Sanità, Rome, Italy
2 Leica Microsystems S.r.l, Buccinasco, Milano, Italy

Key words
Melaleuca alternifolia, Myrtaceae, tea tree oil, terpinen-4-ol, cytoskeleton, melanoma

received 16.11.2020
revised 15.06.2021
accepted 11.08.2021

Bibliography
Planta Med Int Open 2021; 8: e34–e53
DOI 10.1055/a-1623-2938
ISSN 2509-9264

Georg Thieme Verlag KG, Rüdigerstraße 14,
70469 Stuttgart, Germany

Correspondence
Dr. Giuseppina Bozzuto, PhD
Centro Nazionale per la Ricerca e la Valutazione preclinica e clinica dei Farmaci
Istituto Superiore di Sanità
Viale Regina Elena, 299
00161 Rome
Italy
Tel.: + 39/0649/903 405, Fax: + 39/0649/387 118
giuseppina.bozzuto@iss.it

Supplementary material is available under https://doi.org/10.1055/a-1623-2938.

ABSTRACT

Tea tree oil is an essential oil distilled from the leaves of *Melaleuca alternifolia*, a plant native to Australia. It has been used in traditional medicine for its antiseptic and anti-inflammatory properties to treat various skin conditions and infections. It has also been incorporated into many topical formulations to treat cutaneous infections and speed wound healing. *In vivo* and *in vitro* studies report antiproliferative effects in skin disorders but the molecular mechanisms underlying this effect remain to be still elucidated. In this study MTT assay, scanning electron microscopy-field emission gun, flow cytometry, cell cycle assays, and laser scanning confocal microscopy were utilized to investigate a novel mechanism underlying the antiproliferative effects of tea tree oil and terpinen-4-ol on transformed skin (melanoma) M14 cells. The analysis of the actin cytoskeleton by laser scanning confocal microscopy evidenced a clear action of both essential oil and its main active component on F-actin, which interfered with bundling of actin microfilaments in stress fibers. As for the microtubular network, both tea tree oil and terpinen-4-ol induced a disorganization of the perinuclear cage with the rupture and collapse of microtubules. Finally, they noticeably changed the intermediate filaments architecture by inducing the formation of large vimentin cables. Results obtained in the present study point to the cytoskeleton as a further target of tea tree oil and terpinen-4-ol and could account for the inhibition of proliferation and invasion of skin transformed M14 cells. In our experimental conditions, vimentin intermediate filaments appear to be the cytoskeletal element more affected by the treatments. Moreover, the role of cross-linker proteins in the mechanism of action of tea tree oil has been discussed.

ABBREVIATIONS

ABC	ATP-binding cassette
APC	adenomatous polyposis coli
DPPC	dipalmitoyl phosphatidylcholine
ERM	ezrin, radixin, and moesin
FAs	focal adhesions
IF	intermediate filament
KASH	Klarsicht, ANC-1, and Syne/Nesprin homology
LSCM	laser scanning confocal microscopy
MAPK	mitogen-activated protein kinase
SEM-FEG	scanning electron microscopy-field emission gun
STS	staurosporine
SUN	Sad1 and UNC-84
TTO	tea tree oil

Introduction

TTO is an essential oil distilled from the leaves of *Melaleuca alternifolia* (Maiden & Betche) Cheel (Myrtaceae), a plant native to Australia. It has been used in traditional medicine for its antiseptic and anti-inflammatory properties to treat various skin conditions and infections [1]. It has also been incorporated into many topical formulations to treat cutaneous infections, speed wound healing, and as an ingredient in skin products [1–8]. *In vivo* and *in vitro* studies report antiproliferative effects in tumors and skin disorders [9–17], but the molecular mechanisms underlying this effect remain to be fully elucidated. In 2004, we found that TTO and its main active component terpinen-4-ol were able to impair the growth of human melanoma M14 WT cells. This effect was more evident in the resistant variants (M14 ADR cells), which express high levels of the ABC transporter ABCB1 on the plasma membrane, thus overcoming their resistance to caspase-dependent apoptosis [11]. Biophysical and ultrastructural studies performed on simplified planar model membranes (Langmuir films) mimicking lipid "rafts" allowed us to propose a model of TTO-membrane interaction [18]. Based on this model, the effect exerted by TTO on drug-resistant melanoma cells was mediated by the interaction with the fluid DPPC phase rather than with the more organized "rafts," and this interaction preferentially influences the ATP-independent antiapoptotic activity of ABCB1 localized outside "rafts" [18]. Moreover, we also found that ABCB1 overexpressed on the membrane of M14 ADR cells confers them a more aggressive phenotype when compared to their parental type, and that the increase of invasiveness is mediated by the cooperation of ABCB1 with the CD44 molecule [19]. Later on, we found that TTO and its main active component, terpinen-4-ol, can interfere with the migration and invasion processes of drug-sensitive and drug-resistant melanoma M14 cells impairing the ERM-mediated MAPK signaling pathway [20]. These findings strongly suggested an involvement of cytoskeletal elements in the mechanism of action of *Melaleuca* essential oil. Until now, little or not at all is known about the effect of TTO, terpenes, or essential oils on the cytoskeletal architecture. Thus, in this study, we analyzed the effect of TTO and its main active component terpinen-4-ol on actin microfilaments, microtubules, and vimentin IFs of M14 WT and M14 ADR cells by highly defined optical sectioning with LSCM.

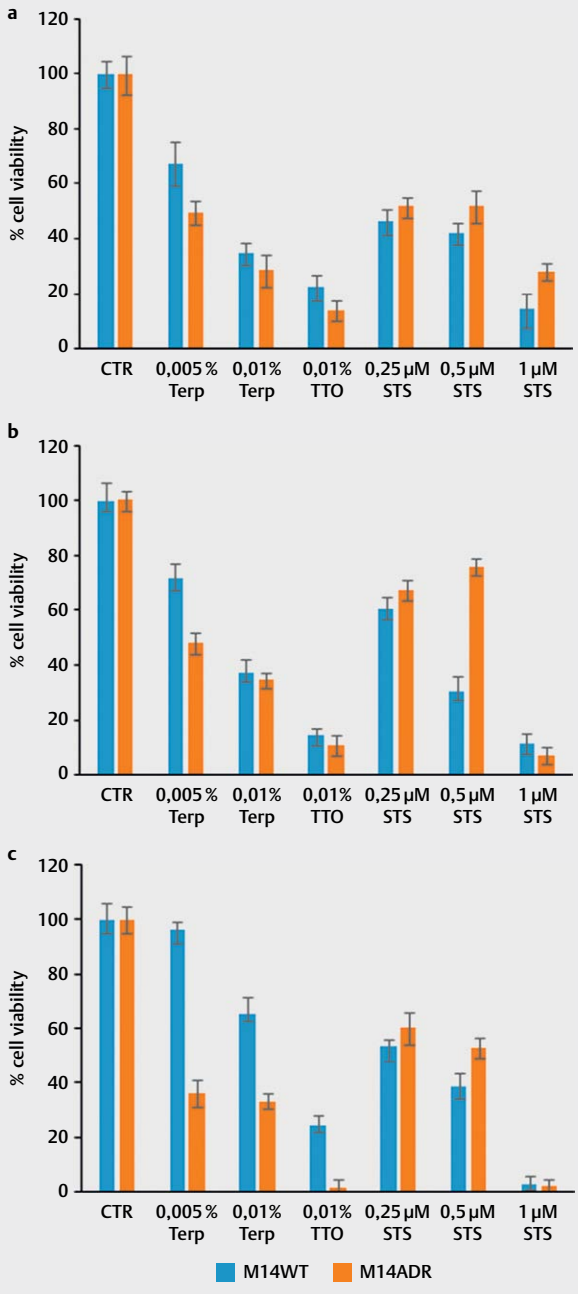

▶ **Fig. 1** Effects of terpinen-4-ol on human melanoma cell viability. The MTT test performed on M14 WT and M14 ADR cells treated with TTO (0.01 %) or terpinen-4-ol (0.005 or 0.01 %) for (**a**) 24 h, (**b**) 48 h, and (**c**) 72 h revealed a dose-dependent decrease in viability of both cell lines. Drug-resistant M14 ADR cells showed to be more sensitive to the effect of both TTO and terpinen-4-ol than their sensitive counterparts. STS (0.25, 0.5, and 1 µM) was used as a positive control of apoptosis induction.

Results and Discussion

The importance of the cytoskeleton in cancer biology is currently recognized and its candidate role as a potential target for cancer treatment is considered today [21]. Actin, microtubule, and vimentin cytoskeletons are retained key players that underpin cancer cellular processes such as cancer cell migration, cell adhesion structures, and metastasis formation [22]. *In vivo* and *in vitro* studies report antiproliferative effects of TTO in tumors and skin disorders [9–17], but the molecular mechanisms underlying this effect remain to be fully elucidated. The effect of TTO and its main active component terpinen-4-ol on the cytoskeletal apparatus has been poorly explored until now.

Sensitivity of drug-sensitive and drug-resistant melanoma cells to tea tree oil and terpinen-4-ol

In our study, firstly, we wanted to confirm the higher sensitivity of human melanoma drug-resistant M14 ADR cells to the cytotoxic action of TTO and its main active component terpinen-4 ol when compared to their drug-sensitive counterpart M14 WT cells [11]. Thus, an MTT assay was performed on M14 ADR cells and their parental M14 WT cells after treatment with TTO (0.01 %) or terpinen-4-ol (0.005 or 0.01 %) for 24, 48, and 72 h. In these experiments, STS was used as a positive control of apoptosis induction. In general, a dose-dependent decrease in viability of both cell lines occurred (▶ **Fig. 1**). As expected, M14 ADR cells appeared to be less sensitive to STS compared to M14 WT cells, but more sensitive to the action of terpinen-4-ol. After exposure of M14 ADR cells to either 0.005 or 0.01 % terpinen-4-ol for 24 (▶ **Fig. 1a**), 48 (▶ **Fig. 1b**), and 72 h (▶ **Fig. 1c**), a decrease in viable cell percentage was observed, greater than that observed in the sensitive counterparts. In particular, in drug-resistant cultures, cell viability decreased 50 % (24 h), 52 % (48 h), and 64 % (72 h) after treatment with 0.005 % terpinen-4-ol, and 71 % (24 h), 66 % (48 h), and 67 % (72 h) after treatment with 0.01 % terpinen-4-ol. M14 WT cells showed a decrease in viable cell percentage of 32 % (24 h), 28 % (48 h), and 4 % (72 h) after exposure to 0.005 % terpinen4-ol, and of 65 % (24 h), 63 % (48 h), and 34 % (72 h) after exposure to 0.01 % terpinen-4-ol. MTT results suggest that, contrarily to M14 ADR cells, drug-sensitive cells were able to recover the damage induced by terpinen-4-ol. With treatment of 0.01 % TTO induced in melanoma cells, a reduction of cell viability percentages greater than that was induced by terpinen-4-ol. Indeed, the exposure to TTO for 24 (▶ **Fig. 1a**), 48 (▶ **Fig. 1b**), and 72 h (▶ **Fig. 1c**) caused a reduction of cell viability percentages of 86, 89, and 98 %, respectively, in M14 ADR cultures and a reduction of 78, 86, and 75 %, respectively, in M14 WT cells. These data confirm that resistant melanoma cells were more sensitive to the treatment with TTO when compared to wild-type cells.

In addition, ultrastructural studies were carried out by SEM in order to analyze, at high resolution, the effect of terpinen-4-ol on the morphology of melanoma cells. SEM analysis showed that untreated M14 WT and M14 ADR cells displayed a characteristic spindle-shaped morphology, with the cell surface covered by numerous and randomly distributed microvilli (▶ **Fig. 2a, b**). Treatment with 0.01 % terpinen-4-ol for 24 h (▶ **Fig. 2c, d**) produced profound morphological alterations. In drug-sensitive cells (▶ **Fig. 2c**), exposure to the *Melaleuca* active component induced the loss of the fusiform shape in some cells, suggesting a reorganization of the underlying cytoskeletal architecture.

However, the effects of terpinen-4-ol were even more devastating in drug-resistant M14 ADR cells: a strong redistribution and clusterization of the microvilli (▶ **Fig. 2d**, arrows) was visible around real holes on the plasma membrane. These results indicated a higher sensitivity of M14 ADR cells to the action of terpinen-4-ol when

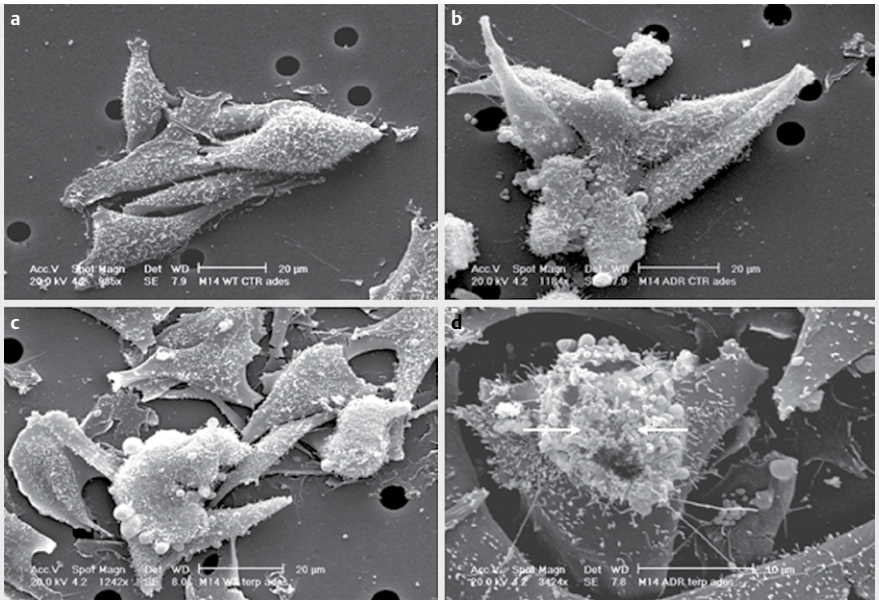

▶ **Fig. 2** Effect of terpinen-4-ol on the morphology of melanoma cells. Ultrastructural studies were carried out by scanning electron microscopy. M14 WT (**a**, **c**) and M14 ADR (**b**, **d**) treated with 0.01 % terpinen-4-ol for 24 h (**c**, **d**). The treatment induced profound morphological alterations with the loss of fusiform morphology (**c**) and formation of holes in the plasma membrane of resistant cells (**d**).

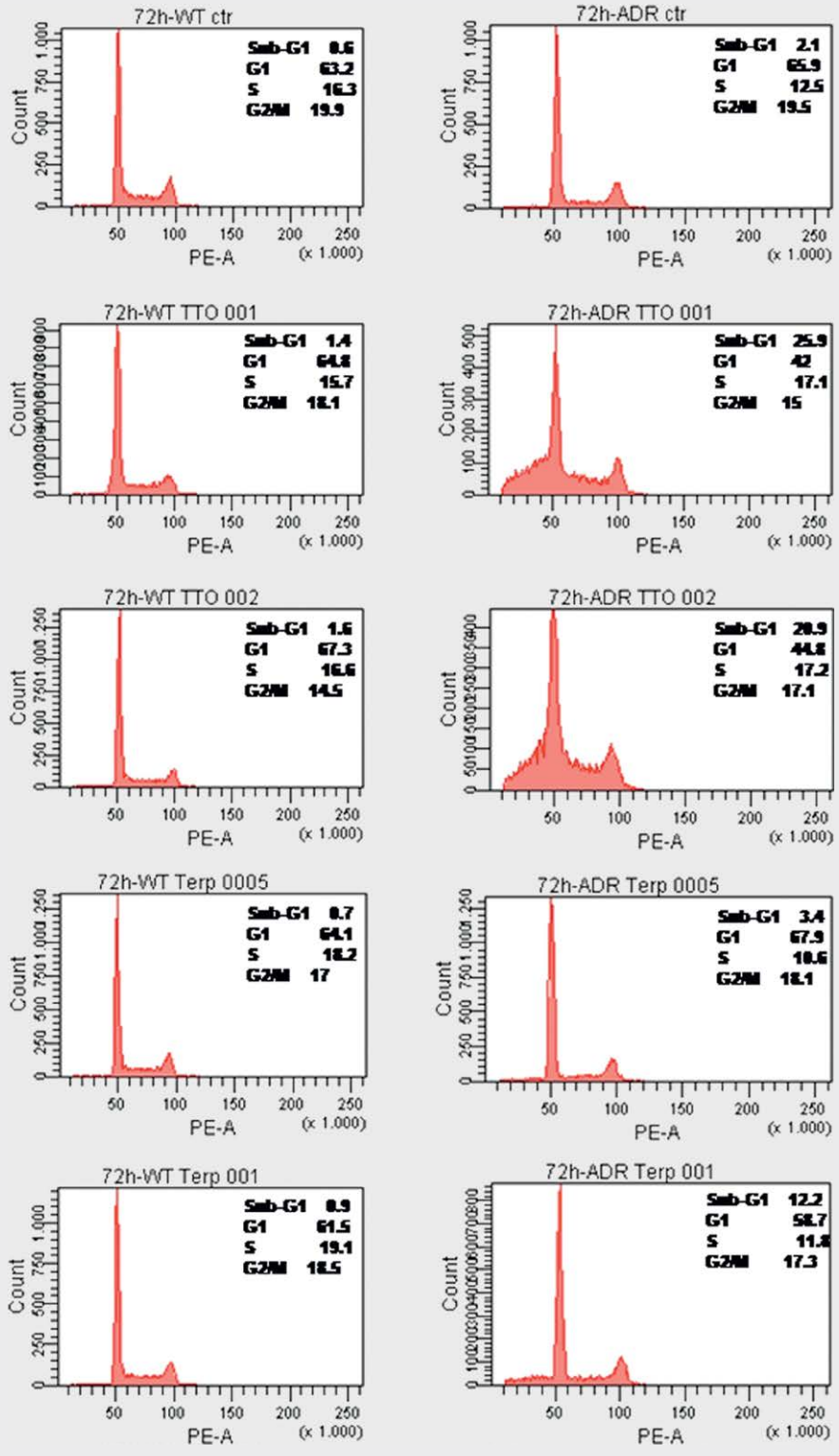

▶ **Fig. 3** Cell cycle analysis performed by flow cytometry on sensitive and drug-resistant M14 cells after treatment for 24, 48, and 72 h with TTO (0.01 and 0.02 %) and terpinen-4-ol (0.005 and 0.01 %). .

compared to the wild-type cells, yet after 24 h of interaction with the active component.

Further, a flow cytometric cell cycle analysis was performed on sensitive and drug-resistant M14 cells after treatment for 24, 48, and 72 h with TTO (0.01 and 0.02 %) and terpinen-4-ol (0.005 and 0.01 %). In M14 WT cells, treatments did not induce significant alterations in cell cycle distribution. Instead, M14 ADR cells showed to be more sensitive than their sensitive counterparts. Even at 24 h, TTO and terpinen-4-ol treatments induced a cytotoxic effect, as a 2- to 3-fold increase of the sub-G1 apoptotic peak was observed in respect to untreated samples, depending on the concentrations (Figs. 1S and 2S, Supporting Information). At longer times, the apoptotic cell population increased to 25.9 and 20.9 % (after 0.01 and 0.02 % TTO treatment, respectively) and to 3.4 and 12.2 % (after with 0.005 and 0.01 % terpinen-4-ol treatment, respectively) (▶ **Fig. 3**).

Thus, cell cycle analysis further confirmed the higher sensitivity of M14 ADR cells to both terpinen-4-ol and the entire mixture of TTO. The observations by high-resolution SEM substantiated the strong interaction of terpinen-4-ol with the plasma membrane of drug-resistant cells, which is in accordance with previous data obtained by biophysical and ultrastructural studies [18]. Furthermore, morphological modifications observed on both M14 WT and M14 ADR cells strongly suggested an involvement of the cytoskeletal apparatus in the cell adaptation and response to the main active component.

Thus, we analyzed the effects of TTO and terpinen-4-ol on the cytoskeleton architecture of M14 melanoma cells using LSCM. The purpose of these observations was to verify if cytoskeletal elements were involved in the mechanism of action of *Melaleuca* essential oil and its active component terpinen-4-ol. We chose the subcytotoxic concentration of terpinen-4-ol employed in the MTT test and cell cycle analysis (0.005 %) and the relative amount present in the en-

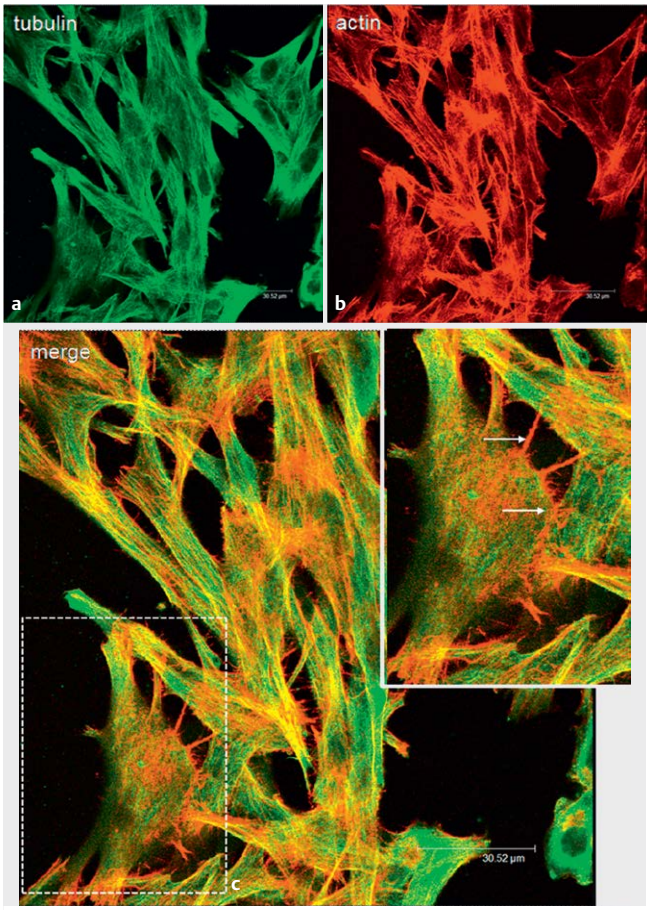

▶ **Fig. 4** LSCM observations of actin and microtubules architecture of untreated M14 WT cells at 24 h from seeding. (**a**) Microtubules labeled with anti-α- and β-tubulin antibodies (green) and (**b**) F-actin microfilaments labeled with TRITC-conjugated phalloidin (red) (**c**) merge (tubulin: green; actin: red; yellow: colocalization). Microtubules radiate out from the microtubule-organizing center, forming a network around the nucleus and extending much of the length and breadth of the cell (**a**). Actin cytoskeleton is organized in stress fibers. F-actin connected with filopodia and microvilli was visible (**b**, **c** and insert, arrows).

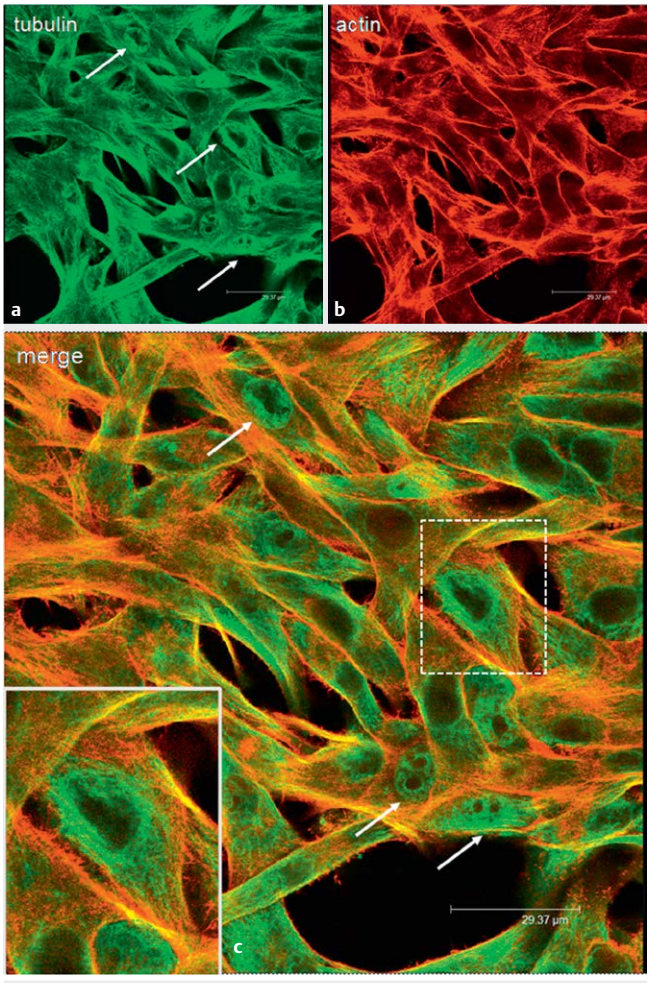

▶ **Fig. 5** LSCM observations of actin and microtubules architecture of M14 WT after treatment with 0.01 % TTO for 24 h. (**a**) Microtubules labeled with anti-α- and β-tubulin antibodies (green) and (**b**) F-actin microfilaments labeled with TRITC-conjugated phalloidin (red) (**c**) merge (tubulin: green; actin: red; yellow: colocalization). After treatment with TTO, stress fibers became less evident; modification of the tubulin network around the nucleus was visible (**a**, **c**, insert and arrows).

tire mixture of TTO (0.01 %) in order to reveal the eventual early alterations of the cytoskeletal elements. All the images are relative to a single confocal section.

Effect of tea tree oil and terpinen-4-ol on actin and tubulin cytoskeleton

Double labeling experiments of both F-actin and α- and β-tubulin allowed to simultaneously highlight the effect of TTO and terpinen-4-ol on actin microfilament and microtubule architecture.

Untreated M14 WT cells displayed an actin cytoskeleton organized in stress fibers, ruffles, and actin connected with microvilli (▶ **Fig. 4b, c**, and insert, arrows). After treatment with TTO (▶ **Fig. 5b**) or terpinen-4-ol (▶ **Fig. 6b**) for 24 h, the stress fibers became less evident. Modifications of the cytoskeletal architecture induced by TTO and terpinen-4-ol were also visible in the tubulin network. In untreated M14 WT cells (▶ **Fig. 4a**), microtubules radiate out from the microtubule-organizing center, forming a network around the nucleus and extending much of the length and breadth of the cell. After treatment with TTO, alterations affecting the perinuclear cage structure were visible (▶ **Fig. 5a, c**, insert, arrows), and even more evident in cells treated with terpinen-4-ol (▶ **Fig. 6a, c** and ▶ **Fig. 7**, inserts, arrows).

Untreated drug-resistant variant M14 ADR cells exhibited an actin cytoskeleton organized in stress fibers (▶ **Fig. 8b, c**) almost identical to those of the sensitive counterpart M14 WT cells. After treatment with TTO or terpinen-4-ol for 24 h (▶ **Figs. 9b** and ▶ **10b**, respectively), the stress fibers were not visible anymore. The microtubule network showed alterations in proximity of the nuclei (▶ **Fig. 9a, c** and ▶ **Fig. 10a, c**, respectively).

After 48 h, the effects of TTO and terpinen-4-ol were still visible. Indeed, in drug-sensitive cells, treatment with TTO and terpinen 4-ol induced the disappearance of the stress fibers (▶ **Figs. 12b** and ▶ **13b**, respectively), which was instead clearly evident in M14 WT control cells (▶ **Fig. 11b, c**). Alterations of the microtubular network around the nuclei were still visible in cells treated with both

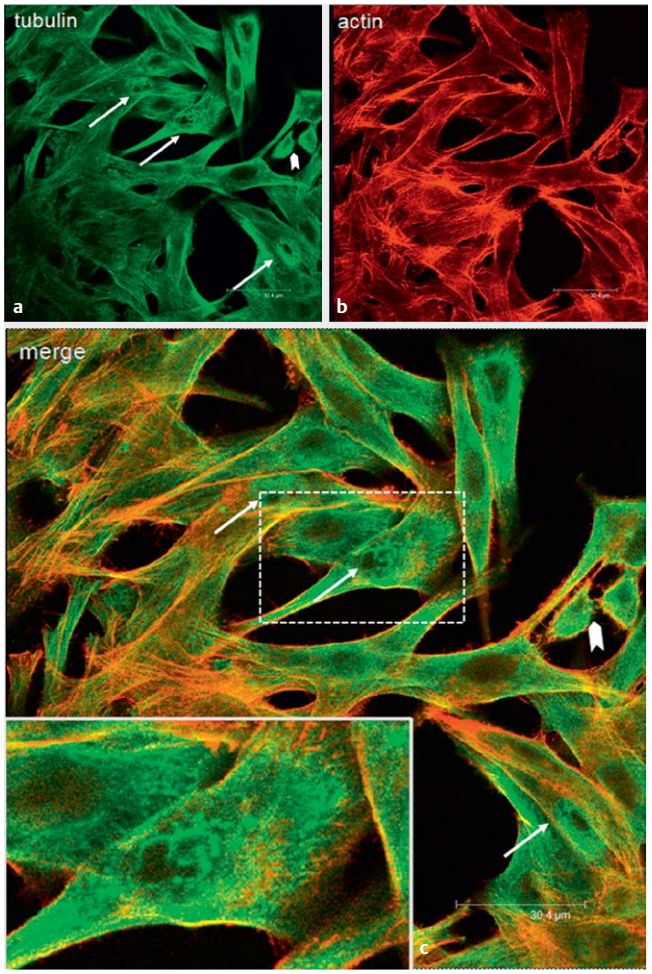

▶ **Fig. 6** LSCM observations of actin and microtubules architecture of M14 WT after treatment with 0.005 % terpinen-4-ol for 24 h. **a** Microtubules labeled with anti-α- and β-tubulin antibodies (green) and **b** F-actin microfilaments labeled with TRITC-conjugated phalloidin (red) **c** merge (tubulin: green; actin: red; yellow: colocalization). After treatment with.005 % terpinen-4-ol stress fibers became less evident (**b**) and alterations of the tubulin network around the nucleus were clearly detected (**a**, **c**, insert and arrows).

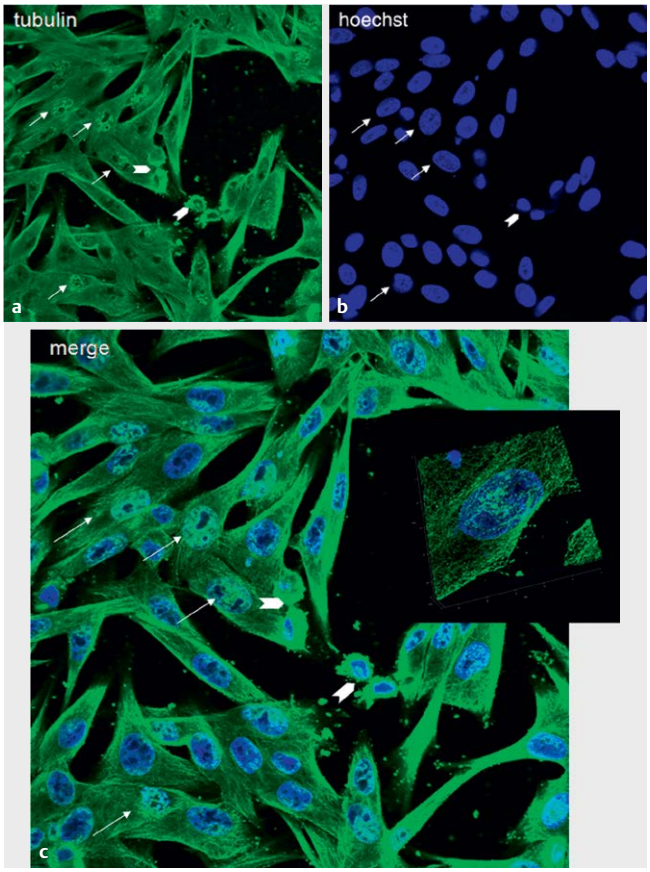

▶ **Fig. 7** LSCM observations of microtubules architecture of M14 WT after treatment with 0.005 % terpinen-4-ol for 24 h **a** Microtubules labeled with anti-α- and β-tubulin antibodies (green). **b** Nuclei labeled with Hoechst. Alterations of the tubulin network around the nuclei were visible (**a**, **c** and insert, arrows). Arrow heads: dividing cells. Insert: 3D maximum intensity reconstruction.

the essential oil (▶ **Fig. 12a, c**, inserts) and its main active component (▶ **Fig. 13a, c**, inserts).

In M14 ADR cells, the damage induced by TTO and terpinen-4-ol on both actin and microtubule networks lasted over the time (▶ **Figs. 15** and ▶ **16**, respectively). Dramatic alterations of cell morphology and depolymerization of F-actin were seen in drug-resistant cells treated with TTO (▶ **Fig. 15b**) and terpinen-4-ol (▶ **Fig. 16b**) when compared to control cells (▶ **Fig. 14b**). Collapse and alterations of microtubules of the nuclear cage were confirmed and clearly visible in both TTO- (▶ **Fig. 15a, c**, inserts) and terpinen-4-ol-treated resistant cells. In the latter, thick microtubule bundles and strongly fluorescent accumulations were observed (▶ **Fig. 16a, c**, inserts).

After 72 h, M14 WT cells recovered from the TTO-induced damage of both actin and tubulin cytoskeletons In fact, TTO-treated cells showed stress fibers (▶ **Fig. 18b, c**) similar to those observed in the control cells (▶ **Fig. 17b, c**) while they still appeared less evident in cells treated with terpinen-4-ol (▶ **Fig. 19b, c**). This recovery was also found at the level of the microtubular network of TTO-treated cells (▶ **Fig. 18a**), which showed a tubulin architecture almost identical to that of the control cells (▶ **Fig. 17a**).

At 72 h, M14 ADR cells recovered the actin damage induced by TTO (▶ **Fig. 21b, c**) but not that induced by terpinen-4-ol (▶ **Fig. 22b, c**). Quite completely reconstituted stress fibers and the microtubular nuclear network were indeed found in resistant TTO-treated cells, which recovered their morphology (▶ **Fig. 21**). Conversely, damages by terpinen-4-ol on F-actin microfilament, microtubules, and cell morphology persisted over time (▶ **Fig. 22**).

The analysis of the actin cytoskeleton by LSCM evidenced a clear action of the essential oil and the main active component on F-ac-

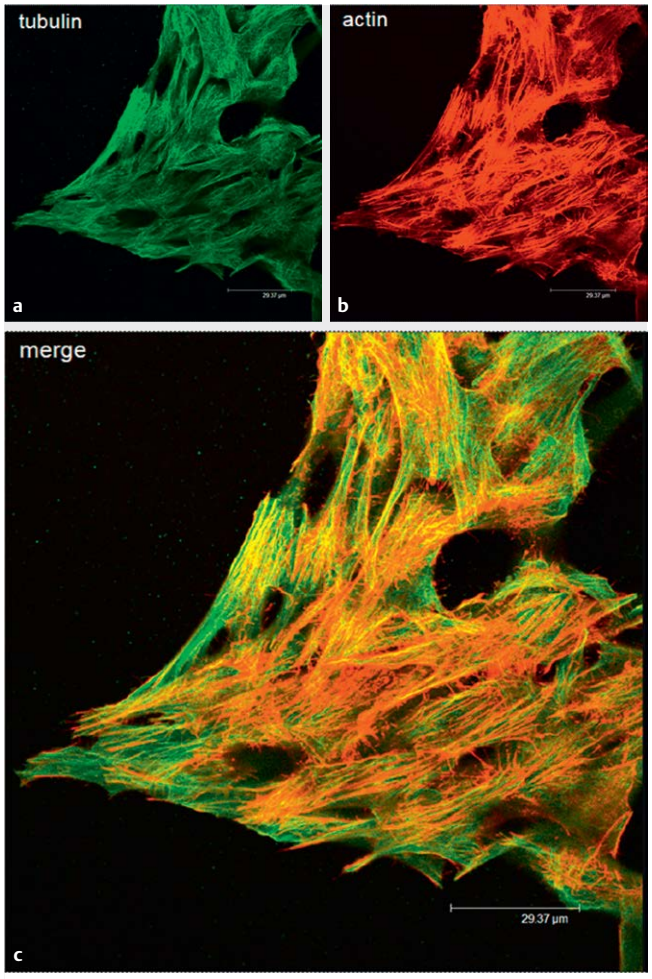

▶ **Fig. 8** LSCM observations of actin and microtubules architecture of untreated M14 ADR cells 24 h from seeding. **a** Microtubules labeled with anti-α- and β-tubulin antibodies (green) and **b** F-actin microfilaments labeled with TRITC-conjugated phalloidin (red) **c** merge (tubulin: green; actin: red; yellow: colocalization). Microtubules form a network around the nucleus and extend outward to the cell periphery (**a**). Similar to wild-type cells, drug-resistant cells displayed an actin cytoskeleton organized in stress fibers (**b**).

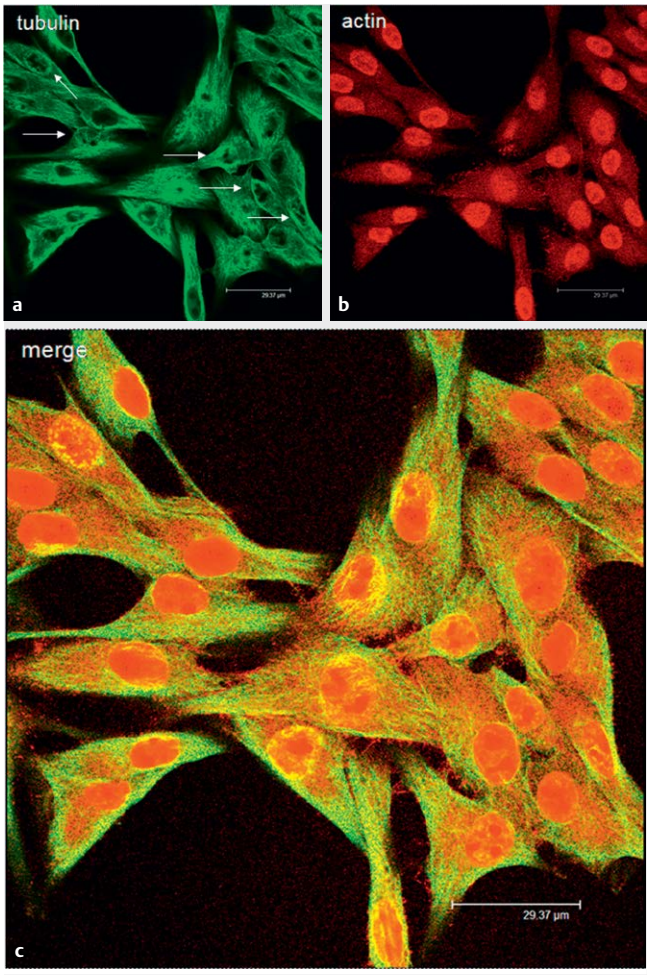

▶ **Fig. 9** LSCM observations of actin and microtubules architecture of M14 ADR cells after treatment with 0.01 % TTO for 24 h. **a** Microtubules labeled with anti-α- and β-tubulin antibodies (green) and **b** F-actin microfilaments labeled with TRITC-conjugated phalloidin (red) **c** merge (tubulin: green; actin: red; yellow: colocalization). Treatment with TTO induced the alteration of the perinuclear tubulin network (**a**, arrows) and the disappearance of the stress fibers (**b**).

tin. Indeed, the treatment with both TTO and terpinen-4-ol induced the disappearance of the stress fibers in both M14 WT and M14 ADR cells. Actin filaments are, in contrast to intermediate filaments and microtubules, semi-flexible filaments, forming dendritic or cross-linked structures [23, 24]. Actin itself is considered the most dynamic of the three cytoskeletal proteins capable of strong structural changes in the time scale of minutes, thus determining the shape of a cell.

Besides globular and filamentous actins (G- and F-actin), there are actin bundles and networks, such as submembrane actin cortex, linked together by cross-linkers, and molecules that connect single actin filaments either transiently or non-transiently. In cell cultures with stiff substrates, the actin cytoskeleton tends to organize in "stress fibers" (dorsal, transverse arcs, ventral), which are bundles of actin filaments cross-linked by an actin-binding protein such as fascin and tensed by myosin II molecular motors [25–28].

In M14 WT and M14 ADR cells treated with essential oil and terpinen-4-ol, stress fibers were not detectable anymore, whereas a fluorescent signal lining plasma membrane and a diffuse weak fluorescence in the cytoplasm were revealed. These observations suggested that in our experimental conditions, TTO and terpinen-4-ol were able to interfere with the bundling of microfilaments in stress fibers. Conversely, disaggregation of the actin cortex did not seem to occur, since fluorescein phalloidin recognized F-actin in proximity of the cell membrane. Moreover, adherent cells with lost stress fibers generally maintained their shape, suggesting that other cytoskeletal elements contributed to maintaining the anchoring of the cells to the substrate. Functional and structural interconnections between actin, microtubules, and IFs are well known. The tight association of the actin cytoskeleton with cell adhesive structures has been largely studied [23]. Both actin fibers and intermediate filaments can guide microtubules to the cell periphery and may contribute to microtubule localization at the rim of FAs

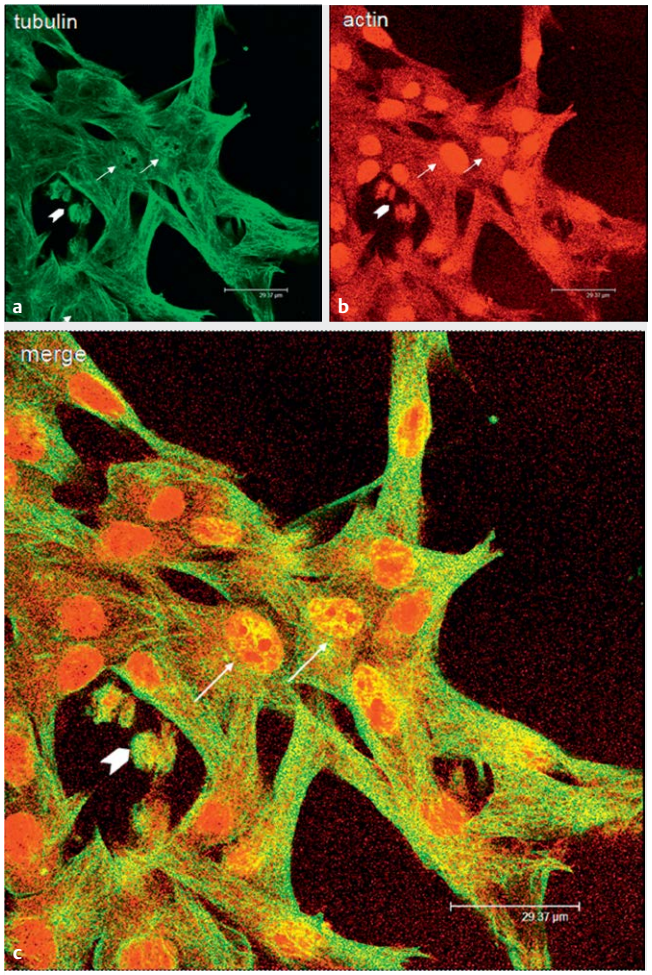

▶ **Fig. 10** LSCM observations of actin and microtubules architecture of M14 ADR cells after treatment with 0.005 % terpinen-4-ol for 24 h. **a** Microtubules labeled with anti-α- and β-tubulin antibodies (green) and **b** F-actin microfilaments labeled with TRITC-conjugated phalloidin (red) **c** merge (tubulin: green; actin: red; yellow: colocalization). Treatment with terpinen-4-ol induced the alteration of the perinuclear tubulin network (**a**, **c**, arrows) and the disappearance of the stress fibers (**b**) .

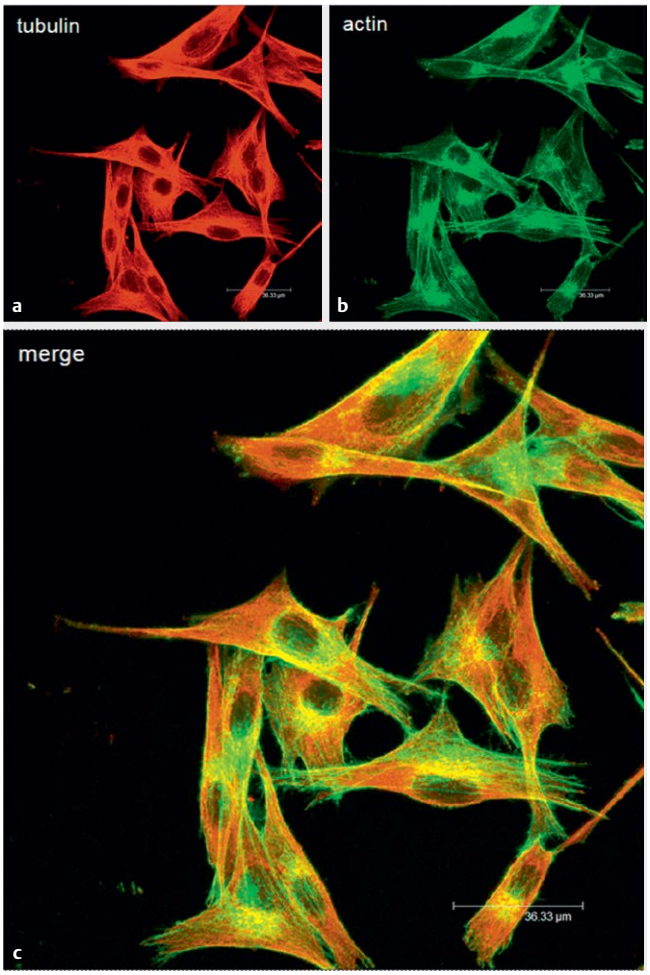

▶ **Fig. 11** LSCM observations of actin and microtubules architecture of untreated M14 WT cells 48 h from seeding. **a** Microtubules labeled with anti-α- and β-tubulin antibodies (red) and **b** F-actin microfilaments labeled with fluorescein-conjugated phalloidin (green) **c** merge (tubulin: red; actin: green; yellow: colocalization). At 48 h, sensitive cells displayed a microtubule (**a**) and microfilament (**b**) pattern similar to that of the 24 h ones. Colocalization areas were visible in perinuclear regions. .

[29, 30]. The physical linkage between vimentin IFs and FAs strengthens the adhesions and promotes their dynamics, boosting the migratory potential of cells [21, 31]. At 72 h, stress fibers were still revealed in M14 WT cells treated with both TTO and terpinen-4-ol and in M14 ADR cells treated with TTO, but not in drug-resistant cells treated with terpinen-4-ol. The irreversible damage induced by terpinen-4-ol on the plasma membrane of M14 ADR cells might further contribute to the loss of actin cytoskeletal integrity.

As far the microtubular network, we found that both TTO and terpinen-4-ol induced a disorganization of the perinuclear cage, which was particularly evident at 48 h, with the rupture and collapse of microtubules. Interactions between the cytoskeleton and the nucleus are well known and affect global cytoskeleton organization. Actin microfilaments, microtubules, and vimentin IFs link the nucleus to the cytoplasmic cytoskeleton via the linker of nucleoskeleton and cytoskeleton complex that is present at the nuclear membrane [32]. Microtubules, actin filaments, and IFs are connected by SUN (inner nuclear membrane) domain and KASH domain (outer nuclear membrane) protein linkers to the nuclear envelope. In particular, actin microfilaments are directly linked to the nucleus by nesprin 1 or nesprin 2, microtubules indirectly by nesprin 4 and kynesin, and IFs indirectly by plectin and nesprin 3, with nesprin proteins being linked to the SUN adaptor protein, localized in the inner membrane and connected to the nuclear lamina. Cytoskeleton links to the nucleus are emerging to be pivotal in various physiological processes, including cell migration, ability for cells to cope with mechanical stress, and altered gene expression profiles [33, 34].

Of note, the damage of the perinuclear cytoskeleton was easily detected in α- and β-tubulin-labeled-treated cells, but not in F-ac-

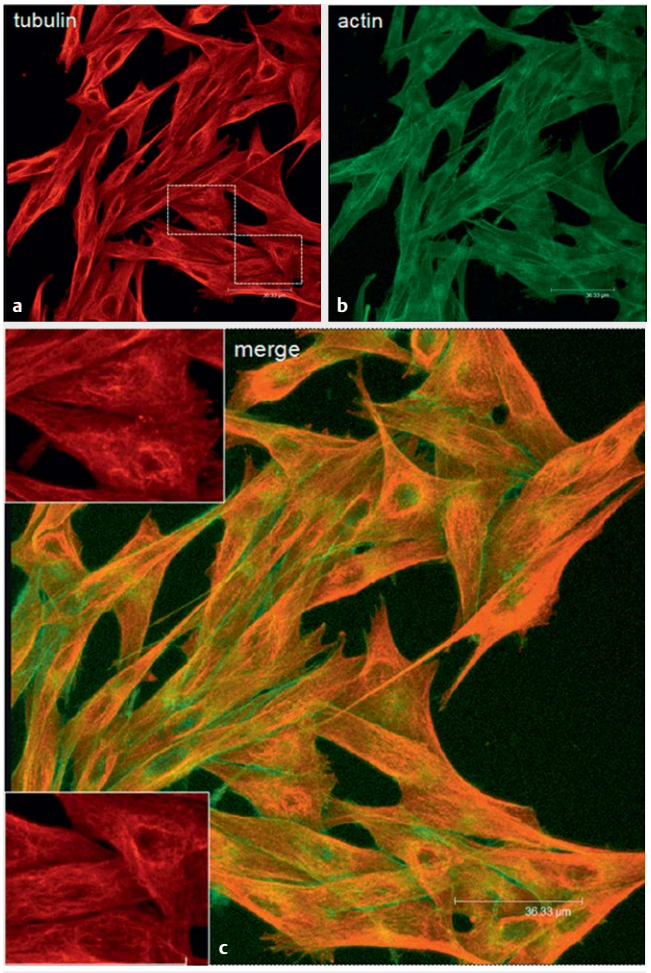

▶ **Fig. 12** LSCM observations of actin and microtubules architecture of M14 WT cells after treatment with 0.01 % TTO for 48 h. **a** Microtubules labeled with anti-α- and β-tubulin antibodies (red) and **b** F-actin microfilaments labeled with fluorescein-conjugated phalloidin (green) **c** merge (tubulin: red; actin: green; yellow: colocalization). Treatment with TTO induced the collapse of the perinuclear microtubules (**a**, **c**, inserts) and the disappearance of the stress fibers and cell organelle-linked F-actin (**b**, **c**).

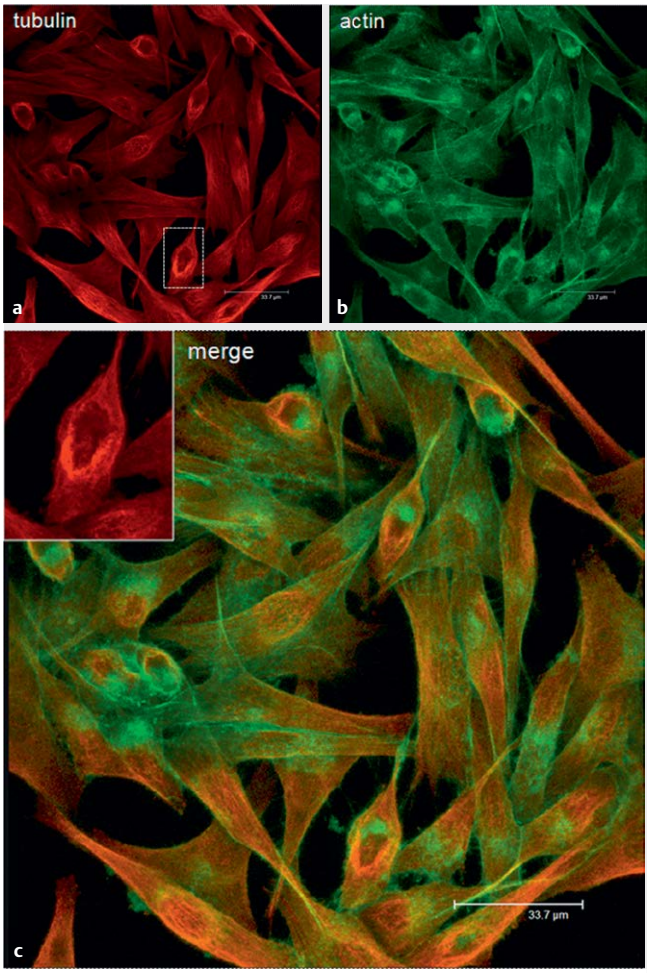

▶ **Fig. 13** LSCM observations of actin and microtubules architecture of M14 WT cells after treatment with 0.005 % terpinen-4-ol for 48 h. **a** Microtubules labeled with anti-α- and β-tubulin antibodies (red) and **b** F-actin microfilaments labeled with fluorescein-conjugated phalloidin (green) **c** merge (tubulin: red; actin: green; yellow: colocalization). Similar to TTO, terpinen 4-ol also induced the collapse of the perinuclear microtubules (**a**, **c**, inserts) and the disappearance of the stress fibers and cell organelle-linked F-actin (**b**, **c**).

tin-labeled cells. However, damage to the perinuclear actin (actin cap) cannot be excluded a priori, since three elements are strictly interconnected by cross-linker proteins such as plectin [35]. On the basis of our observations, we can speculate that the treatments with terpinen-4-ol and TTO induced the detachment and collapse of microtubules from the nuclear envelope.

Effect of tea tree oil and terpinen-4-ol on vimentin intermediate filaments

Vimentin, a major constituent of the IF family of proteins, is ubiquitously expressed in normal mesenchymal cells and is known to maintain cellular integrity and provide resistance against stress. Herein, we report results obtained by LSCM observations on vimentin IFs of both M14 WT and M14 ADR cells after treatment with 0.01 % TTO and 0.005 % terpinen 4-ol for 24, 48, and 72 h. Both M14 WT (▶ **Fig. 23a**) and M14 ADR cells (▶ **Fig. 24a**) showed a robust architecture of vimentin Ifs, with a perinuclear network from which IFs branch out towards the cell periphery. After treatment with TTO for 24 h, an increase of the fluorescence signal was revealed in M14 WT cells (▶ **Fig. 23b**) and M14 ADR cells (▶ **Fig. 24b**). In particular, single IFs appeared to be less resolved and fluorescent vimentin accumulations were revealed (arrows). Forty-eight hours of treatment with TTO and terpinen-4-ol exerted a strong effect in drug-resistant M14 ADR cells (▶ **Fig. 26b**) when compared to their parental counterpart (▶ **Fig. 25b**). Thick vimentin bundles and strongly fluorescent accumulations (arrows) appeared to be clearly detectable. As previously reported, at 72 h from treatment, M14 WT cells recovered the damage induced by TTO, displaying a vimentin pattern similar to that of untreated cells (▶ **Fig. 27**), and a

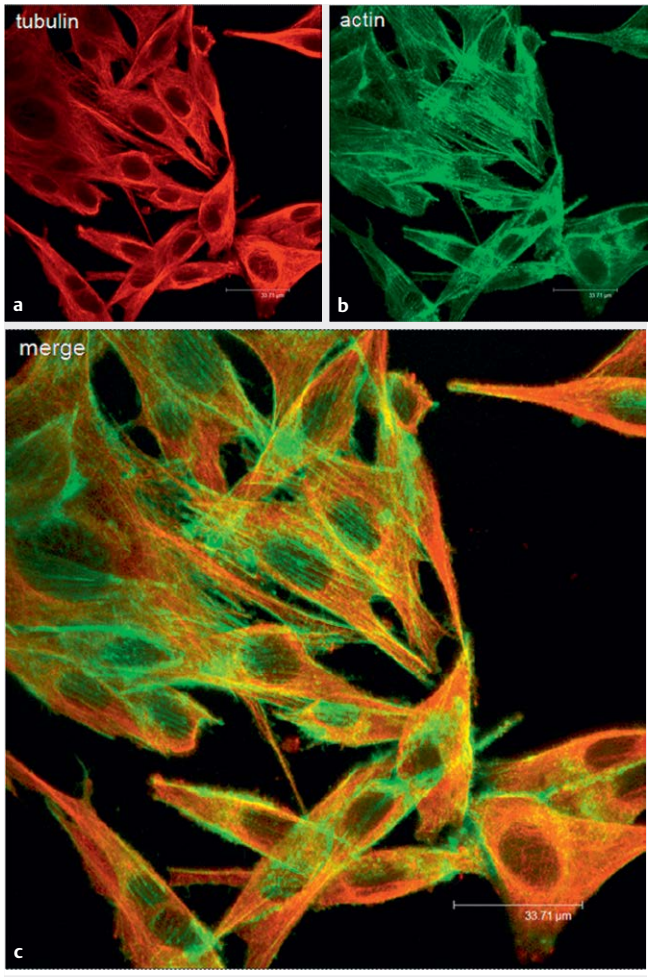

▶ **Fig. 14** LSCM observations of actin and microtubules architecture of untreated M14 ADR cells after 48 h. **a** Microtubules labeled with anti-α- and β-tubulin antibodies (red) and **b** F-actin microfilaments labeled with fluorescein-conjugated phalloidin (green) **c** merge (tubulin: red; actin: green; yellow: colocalization).

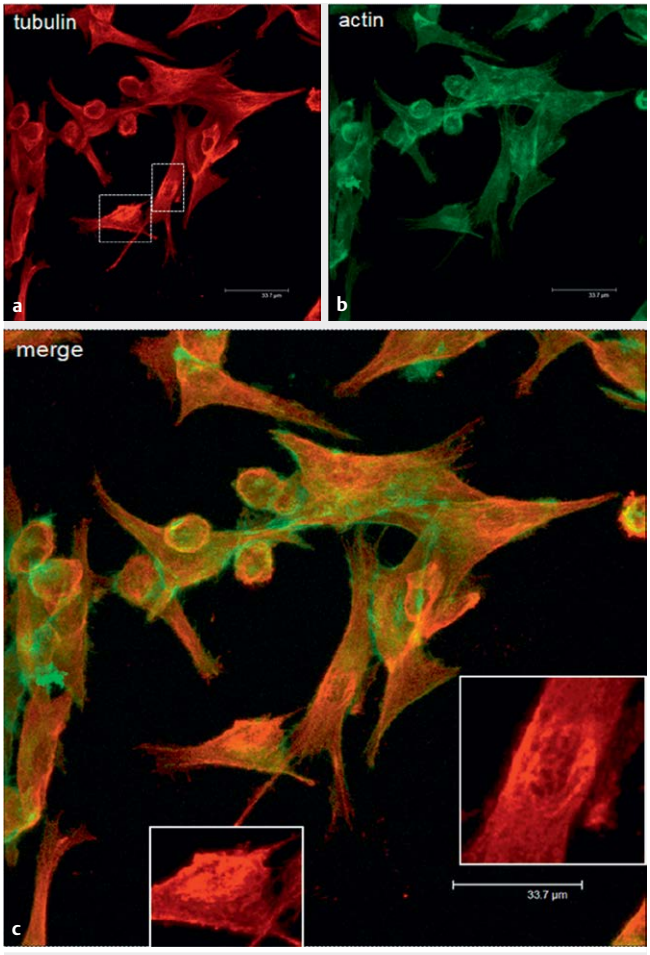

▶ **Fig. 15** LSCM observations of actin and microtubules architecture of M14 ADR cells after treatment with 0.01 % TTO for 48 h. **a** Microtubules labeled with anti-α- and β-tubulin antibodies (red) and **b** F-actin microfilaments labeled with fluorescein-conjugated phalloidin (green) **c** merge (tubulin: red; actin: green; yellow: colocalization). Collapse and alterations of the microtubules of the nuclear cage were confirmed (**a**, **c**, inserts). Dramatic alterations of cell morphology and depolymerization of F-actin were visible (**c**, **b**).

number of mitotic cells was revealed in the cultures (▶ **Fig. 28**). Moreover, single vimentin IFs were more clearly visible. In terpinen-4-ol-treated samples (▶ **Fig. 29**), a number of cells rounded in shape was revealed. Conversely, drug-resistant M14 ADR cells (▶ **Figs. 30–32)** did not recover the cytoskeleton damage. Thick vimentin bundles (arrows) and strongly labeled accumulations (arrows) were still visible in TTO-treated samples (▶ **Fig. 31**). Similarly, in terpinen-4-ol-treated cells (▶ **Fig. 32**), distortion and detachment of IF bundles and strongly fluorescent vimentin accumulations were observable. All these observations denounced that the effect of TTO and its active component terpinen-4-ol persisted over time also on vimentin IFs of drug-resistant cells.

We found that both TTO and terpinen-4-ol noticeably changed the IFs architecture by inducing the formation of strong fluorescent accumulations in the proximity of the nucleus (perinuclear collapse) and vimentin large cables. This alteration appeared still more evident in drug-resistant M14 ADR cells and differently from damages induced on actin and microtubules, irreversible over time both in TTO- and terpinen-4-ol-treated cells.

The vimentin IF network provides a cytoarchitecture with mechanical stability that also enables precise spatiotemporal coordination between all three cytoskeletal components [36]. Vimentin can interact with actin filaments both directly through its C-terminal tail [37] and indirectly through the cytoskeletal cross-linking proteins [35]. More precisely, transverse arcs and ventral stress fibers interact with vimentin IFs through plectin [38]. Vimentin IFs also interact with microtubules through the tumor suppressor APC [39] and indirectly via cross-linking with plectin [35].

In conclusion, results obtained in the present study clearly point out to the cytoskeleton as a further target of *M. alternifolia* and its

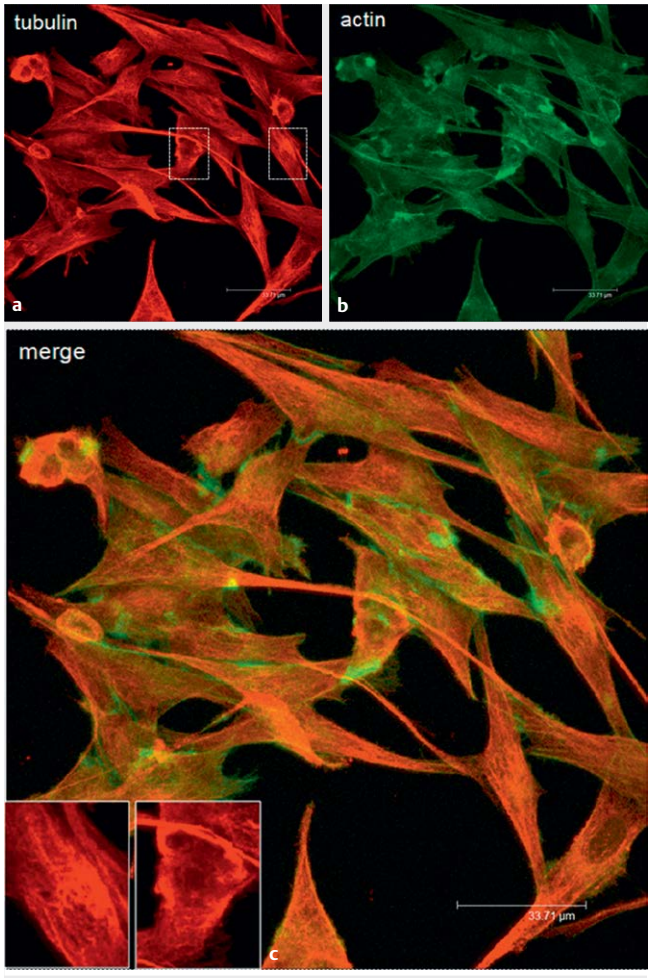

▶ **Fig. 16** LSCM observations of actin and microtubules architecture of M14 ADR cells after treatment with 0.005 % terpinen-4-ol for 48 h. **a** Microtubules labeled with anti-α- and β-tubulin antibodies (red) and **b** F-actin microfilaments labeled with fluorescein-conjugated phalloidin (green) **c** merge (tubulin: red; actin: green; yellow: colocalization). Treatment with terpinen-4-ol induced the collapse of perinuclear microtubules (**a**, **c**, and inserts) and the disappearance of the stress fibers and cell organelle-linked F-actin (**b**, **c**).

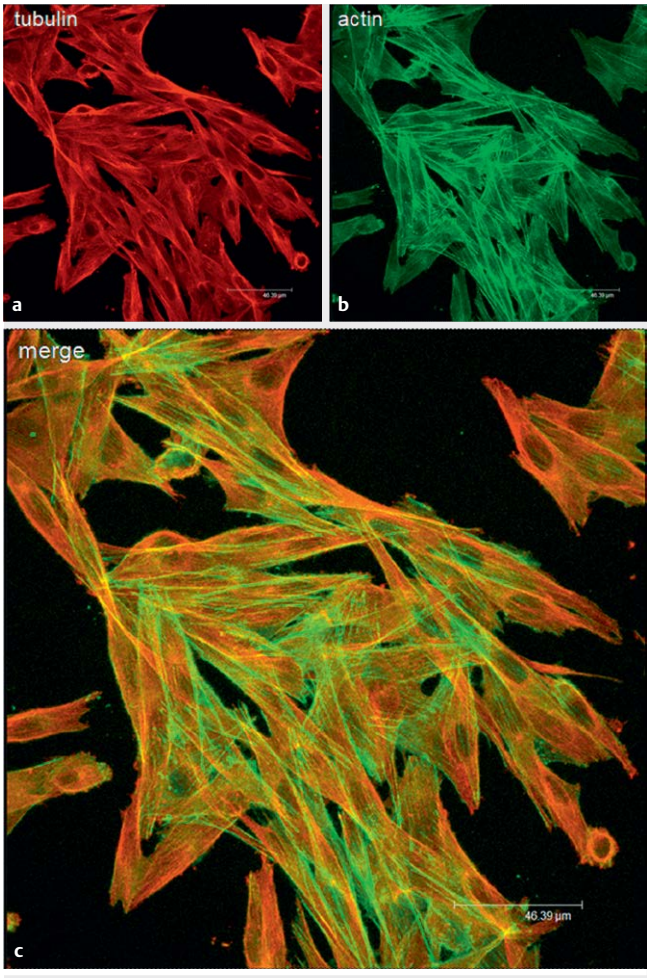

▶ **Fig. 17** LSCM observations of actin and microtubules architecture of untreated M14 WT cells 72 h from seeding. **A** Microtubules labeled with anti-α- and β-tubulin antibodies (red) and **b** F-actin microfilaments labeled with fluorescein-conjugated phalloidin (green) **c** merge (tubulin: red; actin: green; yellow: colocalization). Cells displayed elongated shapes with microfilaments and microtubules running parallel to the long axis of the cell (**a**-**c**).

main active component terpinen-4-ol and could account for the inhibition of proliferation and aggressiveness of drug-resistant M14 cells. Strikingly, the cytoskeletal alterations observed by LSCM on actin, microtubules, and vimentin appeared localized in precise different structures of the cytoskeletal network, i. e., actin stress fibers, tubulin perinuclear cage, and vimentin IF architecture. In our experimental conditions, vimentin IFs appear to be the cytoskeletal element more affected by the treatments. Cross-linker proteins might play a role in the mechanism of action of TTO, and further studies will be carried out in order to better understand this issue.

Materials and Methods

Tea tree oil

TTO was purchased from Variati SPA (batch no. 061220052) and was certified for the following chemical composition: α-pinene 2.5 %, sabinene 0.2 %, α-terpinene 10 %, para cimene 1.9 %, d-limonene 1 %, 1,4-cineole 2.9 %, γ-terpinene 21.2 %, α-terpinolene 3.5 %, terpinen-4-ol 40.3 %, α-terpineol 3.2 %, aromadendrene 1.2 %, δ-cadinene 0.9 %, globulol 0.3 %, and viridiflorol 0.4 %. The analysis was performed by using a gas chromatograph fitted with a flame ionization detector.

Chemicals and reagents

RPMI 1640 medium, penicillin/streptomycin solution 100X, L-glutamine solution 200 nM, and MEM nonessential amino acids 100X

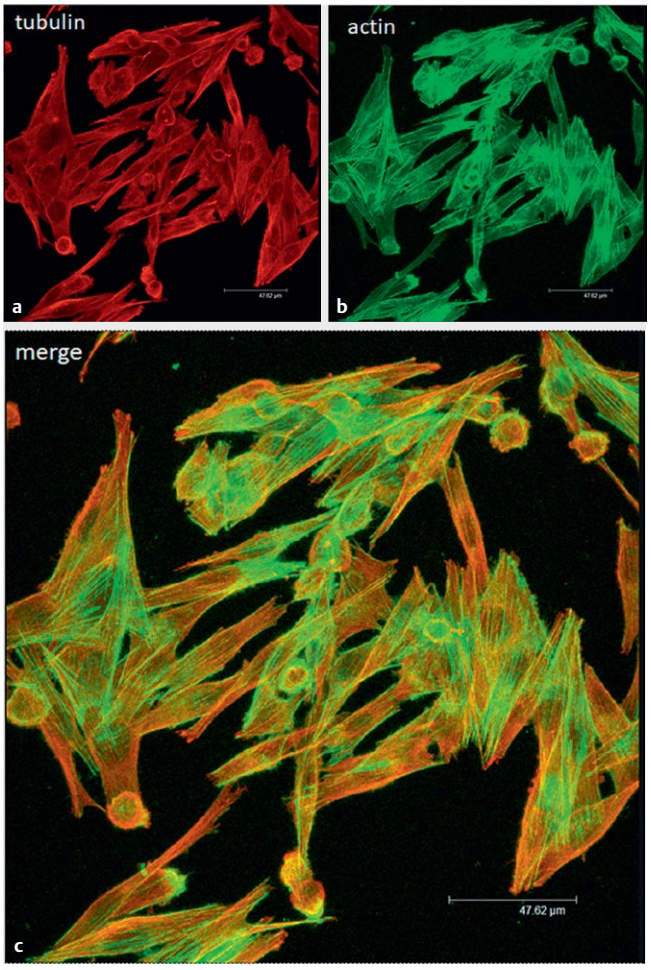

▶ **Fig. 18** LSCM observations of actin and microtubules architecture of M14 WT cells after treatment with 0.01 % TTO for 72 h. **a** Microtubules labeled with anti-α- and β-tubulin antibodies (red) and **b** F-actin microfilaments labeled with fluorescein-conjugated phalloidin (green) **c** merge (tubulin: red; actin: green; yellow: colocalization). M14 WT cells recovered TTO-induced damage of both actin and the tubulin cytoskeleton.

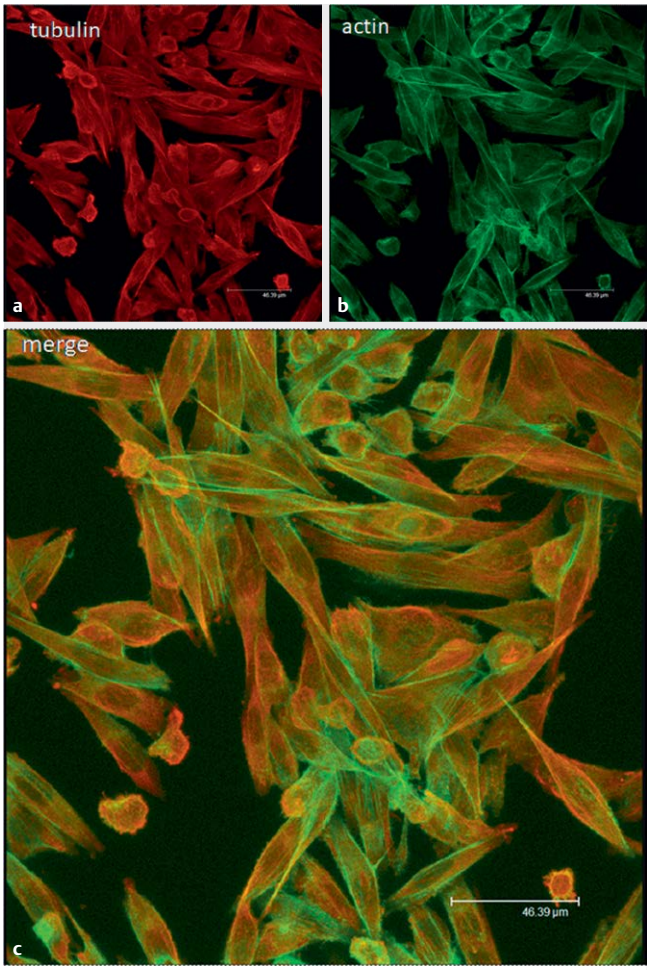

▶ **Fig. 19** LSCM observations of actin and microtubules architecture of M14 WT cells after treatment with 0.005 % terpinen-4-ol for 72 h. **a** Microtubules labeled with anti-α- and β-tubulin antibodies (red) and **b** F-actin microfilaments labeled with fluorescein-conjugated phalloidin (green) **c** merge (tubulin: red; actin: green; yellow: colocalization). M14 WT cells recovered terpinen-4-ol-induced damage of both actin and the tubulin cytoskeleton.

were purchased from EuroClone S.p.A. FBS was purchased from Hyclone. Anti-α- and β-tubulin antibodies, DMSO, MTT, phalloidin TRITC, PBS, ribonuclease, STS, terpinen-4-ol (purity 100 %), and Triton X-100 were purchased from Sigma-Aldrich. Anti-vimentin antibody was purchased from Santa Cruz Biotechnology. Secondary Alexa 488 goat anti-mouse IgG and Alexa 633 goat anti-mouse IgG were purchased from Molecular Probes. Propidium iodide was purchased from Applichem. Glutaraldehyde (25 % acqueous solution) and sodium cacodylate (powder) were purchased from TAAB Laboratories Equipment Ltd. Osmium (VIII) oxide for microscopy was purchased from Merck KGaA.

Cell cultures

The established human melanoma cell lines M14 WT and M14 ADR were grown in RPMI 1640 medium supplemented with 1 % L-glutamine, 1 % nonessential amino acids, 100 IU/mL penicillin/streptomycin, and 10 % FBS at 37 °C in a 5 % CO_2 humidified atmosphere in air. The M14 ADR cell line was selected culturing M14 WT cells in the presence of 40 µM ADR (Adriblastina; Pharmacia & Upjohn S.p.A) as described in Calcabrini et al. [11].

MTT assays

M14 WT and M14 ADR cells were seeded in 96-well plates at a density of 1×10^4 cells/well in complete medium (200 µL). On the following day, cells were treated with TTO (0.01 %) or terpinen-4-ol (0.005 or 0.01 %) in triplicate. STS (0.25, 0.5, and 1 µM) was used as a positive control of apoptosis induction. After 24, 48, and 72 h of treatment, the cell medium was removed, and cells were washed with PBS and incubated with 0.5 mg/mL MTT for 3 h at 37 °C. After removing the MTT solution, the samples were lysed by 100 µL

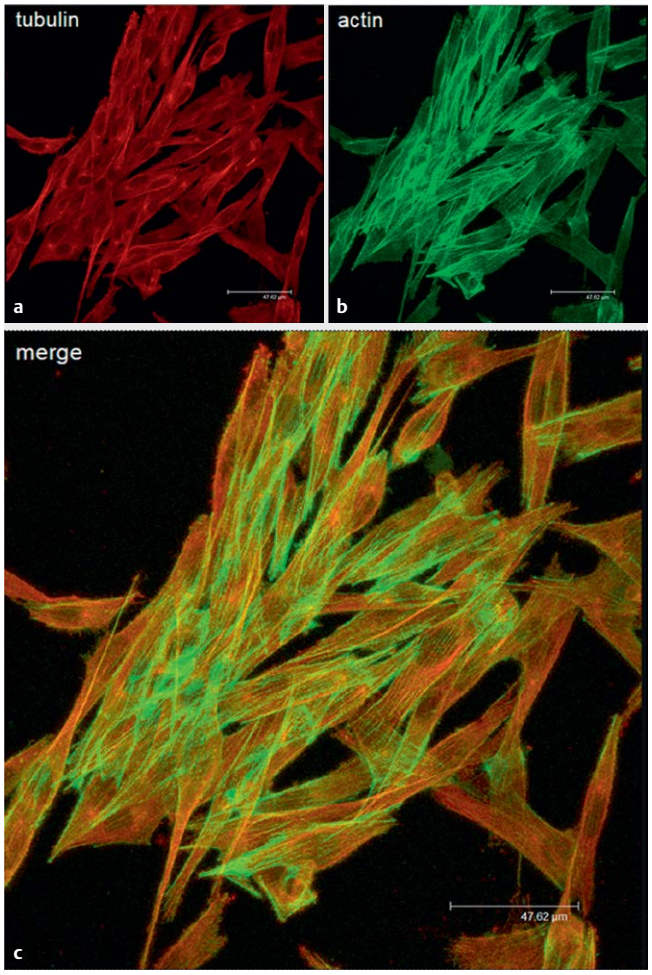

▶ **Fig. 20** LSCM observations of actin and microtubules architecture of untreated M14 ADR cells 72 h from seeding. **A** Microtubules labeled with anti-α- and β-tubulin antibodies (red) and **b** F-actin microfilaments labeled with fluorescein-conjugated phalloidin (green) **c** merge (tubulin: red; actin: green; yellow: colocalization). Similar to wild-type cells, resistant cells displayed elongated shapes with microfilaments and microtubules running parallel to the long axis of the cell (**a**-**c**).

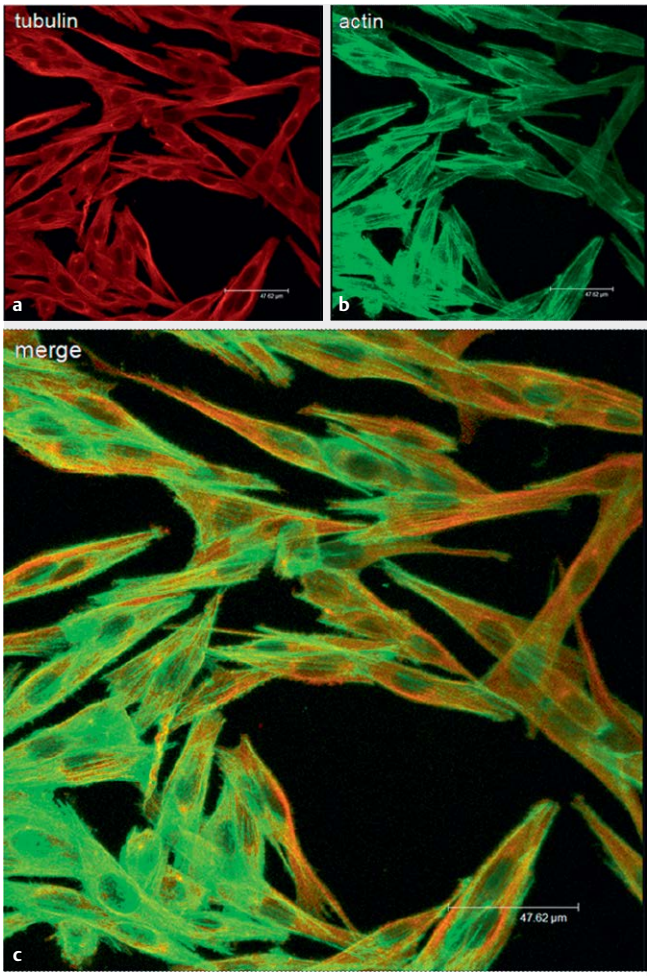

▶ **Fig. 21** LSCM observations of actin and microtubules architecture of M14 ADR cells after treatment with 0.01 % TTO for 72 h. **a** Microtubules labeled with anti-α- and β-tubulin antibodies (red) and **b** F-actin microfilaments labeled with fluorescein-conjugated phalloidin (green) **c** merge (tubulin: red; actin: green; yellow: colocalization). M14 ADR cells recovered the actin damage induced by TTO. Stress fibers and the microtubular nuclear network appeared to be quite completely reconstituted (**a**-**c**).

DMSO and analyzed by a microplate reader (Fusion Universal Microplate Analyzer; Packard) at 570 nm. After normalizing the optical density (OD) of each well to the absorbance value of the blank, the percentage of cell viability was calculated as follow: (OD mean value of the treated sample/OD mean value of the control sample) × 100.

Flow cytometry

For cell cycle analysis, M14 WT and M14 ADR cells were seeded in complete medium (2×10^5 in 6 wells). After 24 h, they were treated with 0.01 % TTO or 0.005 % terpinen-4-ol. After 24, 48, and 72 h, cells were collected, washed twice with cold PBS, and centrifuged. The pellet was fixed in 70 % ethanol and kept at 4 °C until the time of staining with PBS containing 40 µg/mL propidium iodide and 100 µg/mL ribonuclease at 37 °C for 30 min. Samples were then analyzed by a BDLSRII flow cytometer (Becton, Dickinson & Company). Percentages of cells in subG1, G1, S, and G2/M phases were calculated using FACS (Fluorescence-Activated Cell Sorter) Diva Software (Becton, Dickinson & Company).

Scanning electron microscopy

To analyze the effect of terpinen-4-ol on the cell morphology of melanoma cells, 5×10^5 cells were seeded on porous membranes (8.0 µm pore; Falcon) that stood in 6-well plates and were incubated at 37 °C in a 5 % CO_2 humidified atmosphere in air. After 24 h cells were treated with 0.01 % terpinen-4-ol. After 18 h of incubation, samples were fixed with 2.5 % glutaraldehyde in 0.1 M cacodylate buffer (pH 7.3), with 2 % sucrose added, for 30 min at room temperature. After post-fixation with 1 % OsO4 in 0.1 M cacodylate buffer (pH 7.3), cells were dehydrated through a graded ethanol series, critical point-dried in CO_2 (030 Balzers device), and gold coated by sputtering (SCD 040 Balzers device, Bal-Tec). The samples were

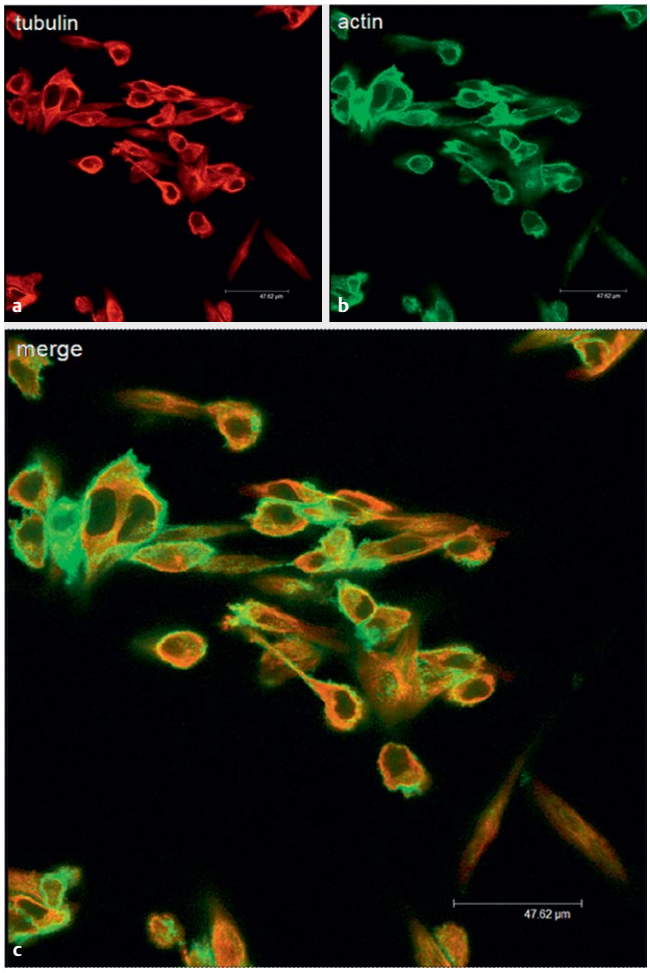

▶ **Fig. 22** LSCM observations of actin and microtubules architecture of M14 ADR cells after treatment with 0.005 % terpinen-4-ol for 72 h. **a** Microtubules labeled with anti-α- and β-tubulin antibodies (red) and **b** F-actin microfilaments labeled with fluorescein-conjugated phalloidin (green) **c** merge (tubulin: red; actin: green; yellow: colocalization). Damages by terpinen-4-ol on the F-actin microfilament, microtubules, and cell morphology persisted over time (**a**-**c**).

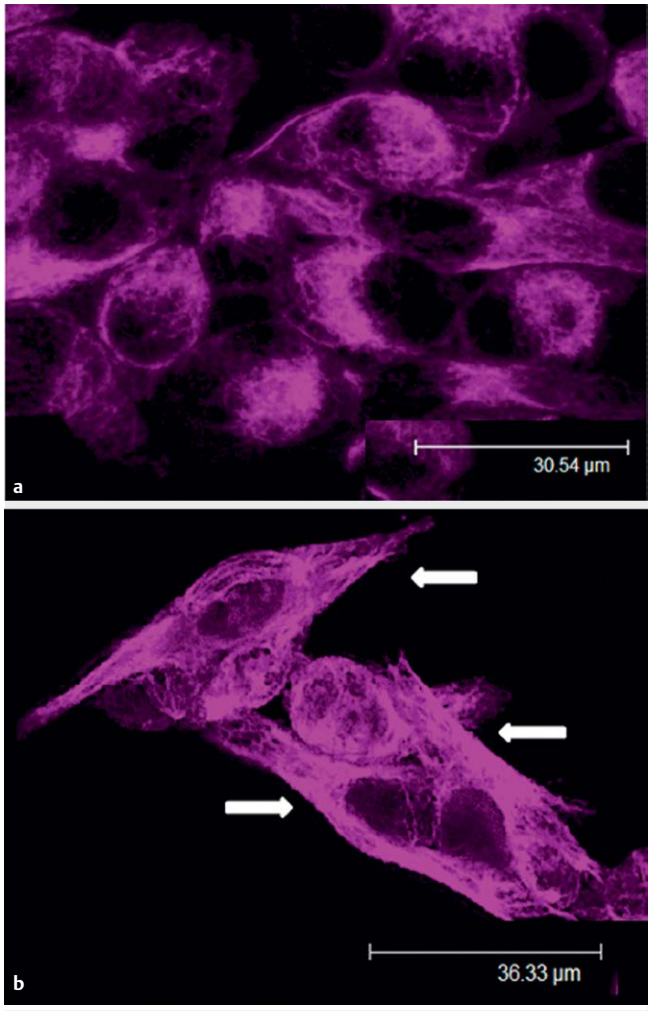

▶ **Fig. 23** LSCM observations of vimentin architecture of M14 WT cells before (**a**) and after treatment with 0.01 % TTO (**b**) for 24 h. Large vimentin bundles or strongly fluorescent accumulations were revealed (**b**, arrows).

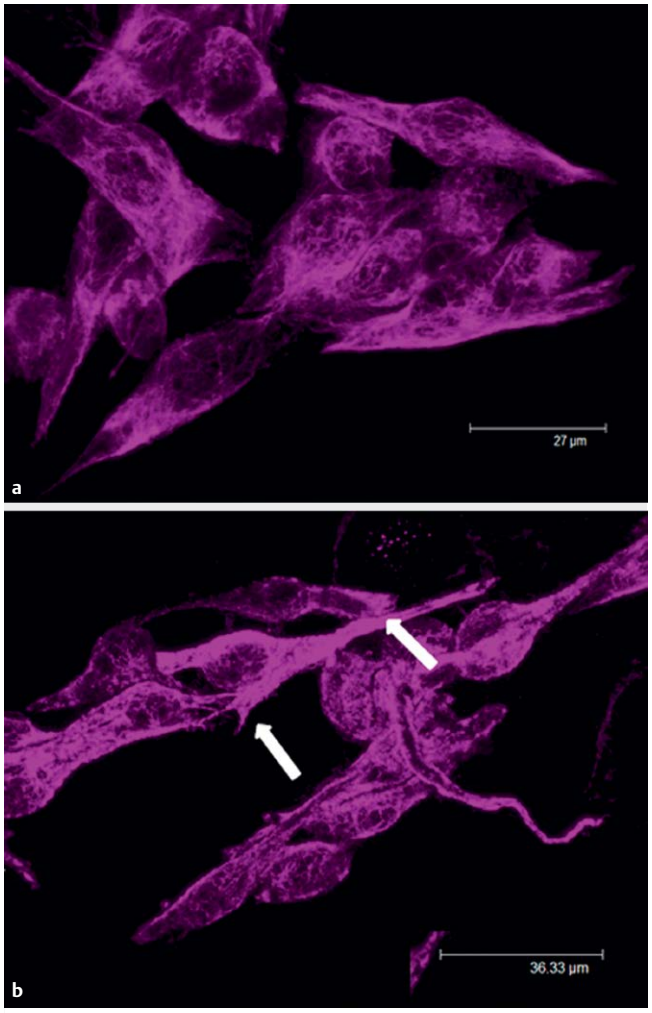

▶ **Fig. 24** LSCM observations of vimentin architecture of M14 ADR cells before (**a**) and after treatment with 0.01 % TTO (**b**) for 24 h. Single Ifs appeared to be less resolved and fluorescent vimentin accumulations in the proximity of nuclei were revealed (**b**, arrows).

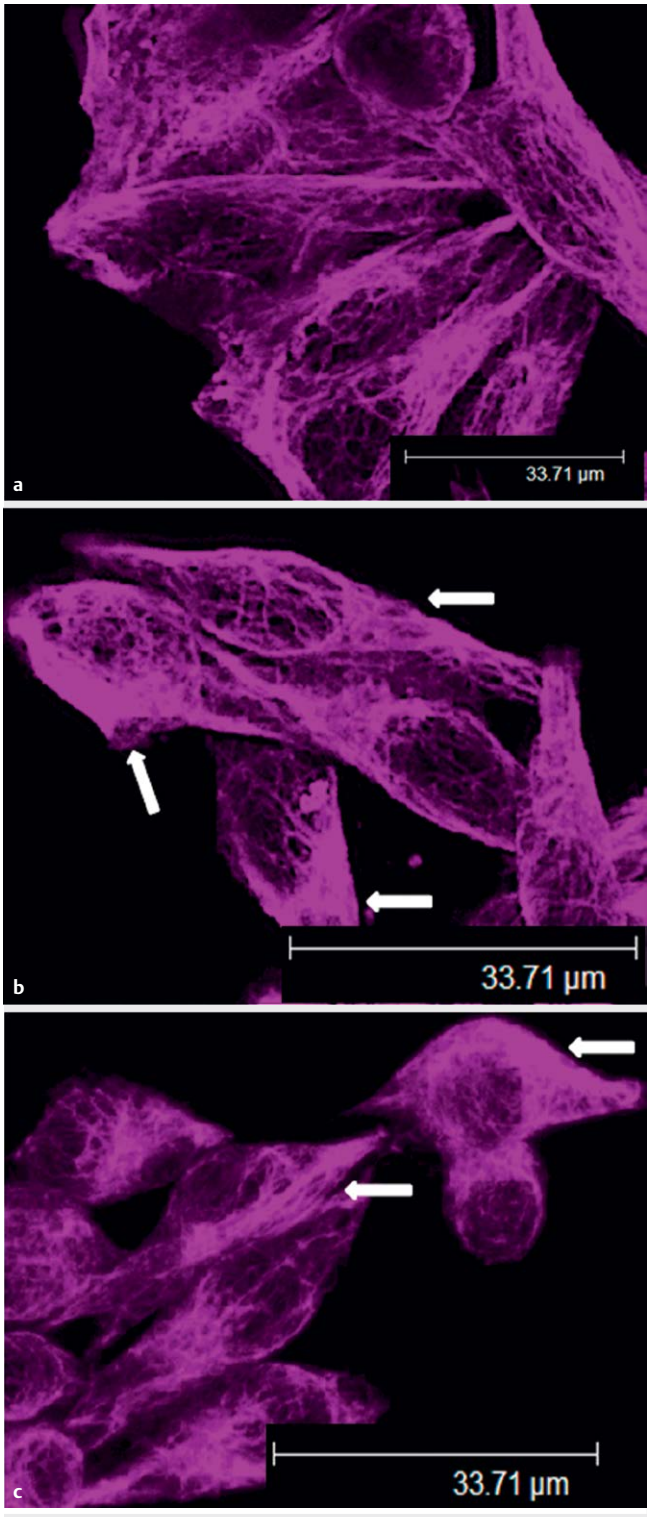

▶ **Fig. 25** LSCM observations of vimentin architecture of M14 WT cells before (**a**) and after treatment with 0.01 % TTO (**b**) or 0.005 % terpinen-4-ol for 48 h. (**c**) Large vimentin bundles or strongly fluorescent accumulations were revealed (**b**, **c**, arrows).

then examined with a SEM-FEG (Quanta 200 Inspect, FEI Company).

Laser scanning confocal microscopy

For immunofluorescence analyses, 5×10^4 cells were seeded in 24-well cluster plates onto 12-mm cover glasses and incubated overnight at 37 °C in a 5 % CO2 humidified atmosphere in air. The next day, the cells were treated with 0.01 % TTO or 0.005 % terpinen-4-ol.

At the end of treatments, for the immunostaining of tubulin and actin, samples were washed with PBS and fixed in 3.7 % paraformaldehyde with 2 % sucrose for 30 min at room temperature. Samples were then washed twice in PBS, permeabilized with 0.5 % Triton X-100 for 5 min, and incubated with a blocking solution (10 %

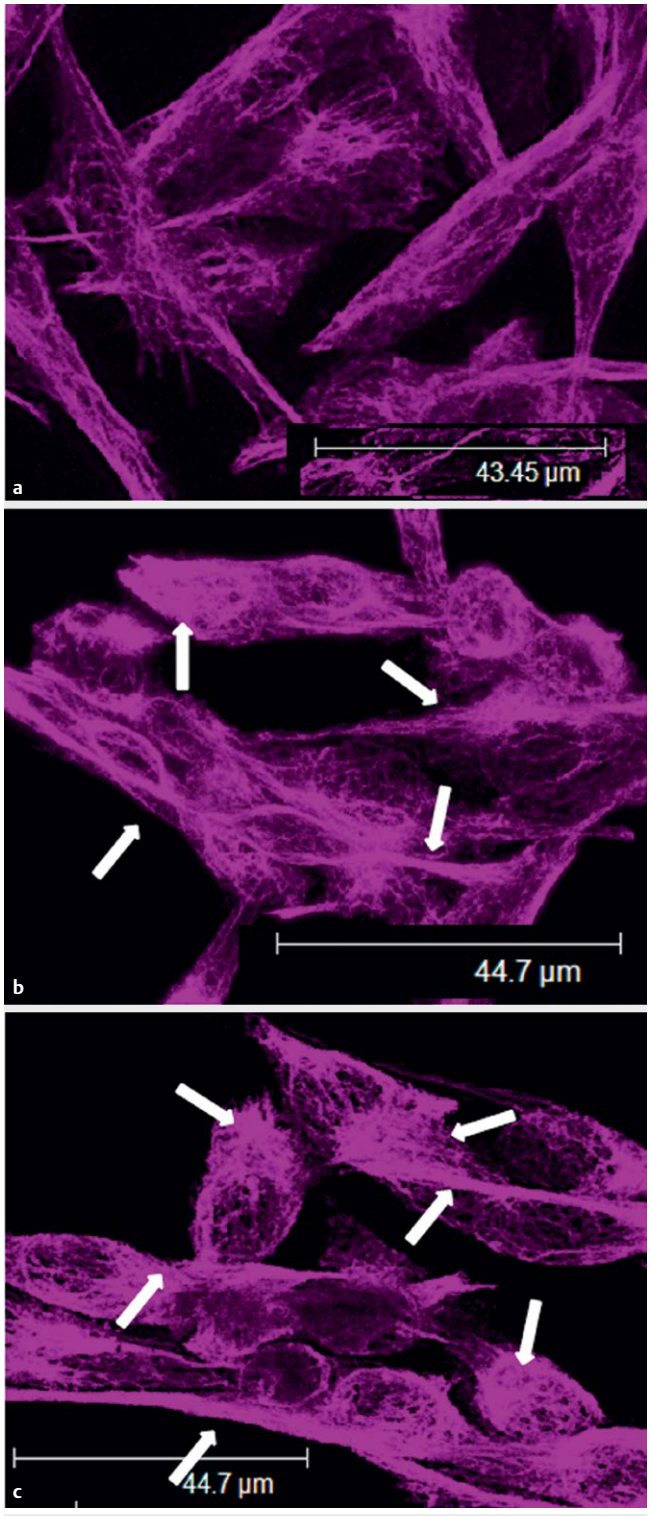

▶ **Fig. 26** LSCM observations of vimentin architecture of M14 ADR cells before (**a**) and after treatment with 0.01 % TTO (**b**) or 0.005 % terpinen-4-ol for 48 h. (**c**) After treatment with TTO and terpinen-4-ol, thick vimentin bundles and strongly fluorescent accumulations (arrows) were clearly detectable.

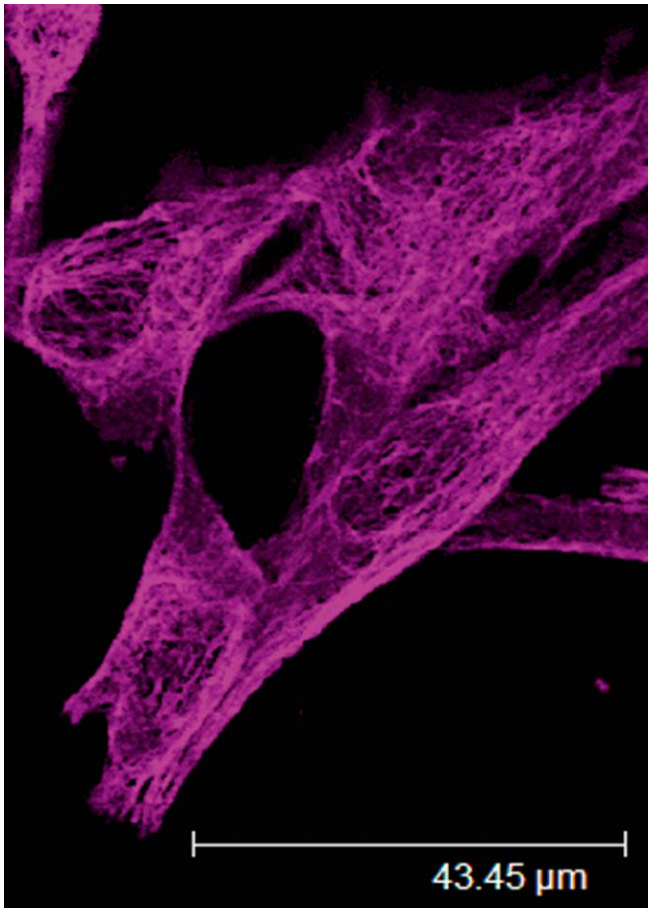

▶ **Fig. 27** LSCM observations of vimentin architecture of untreated M14 WT cells 72 h from seeding.

FBS, 10 % AB serum, 1 % bovine serum albumin in PBS) for 30 min. Microtubule staining was performed by incubating melanoma cells with a mouse monoclonal anti-α/β-tubulin antibody mixture diluted 1:50 in PBS containing 10 % FBS, 10 % AB serum, and 1 % bovine serum albumin for 30 min at room temperature. Samples were then washed in PBS and incubated with a mixture of secondary Alexa 488 goat anti-mouse IgG (1:50) and phalloidin TRITC (1:100) or Alexa 546 goat anti-mouse IgG (1:50) and phalloidin FITC (1:100) for 30 min at room temperature. Cells were rinsed three times with PBS afterwards.

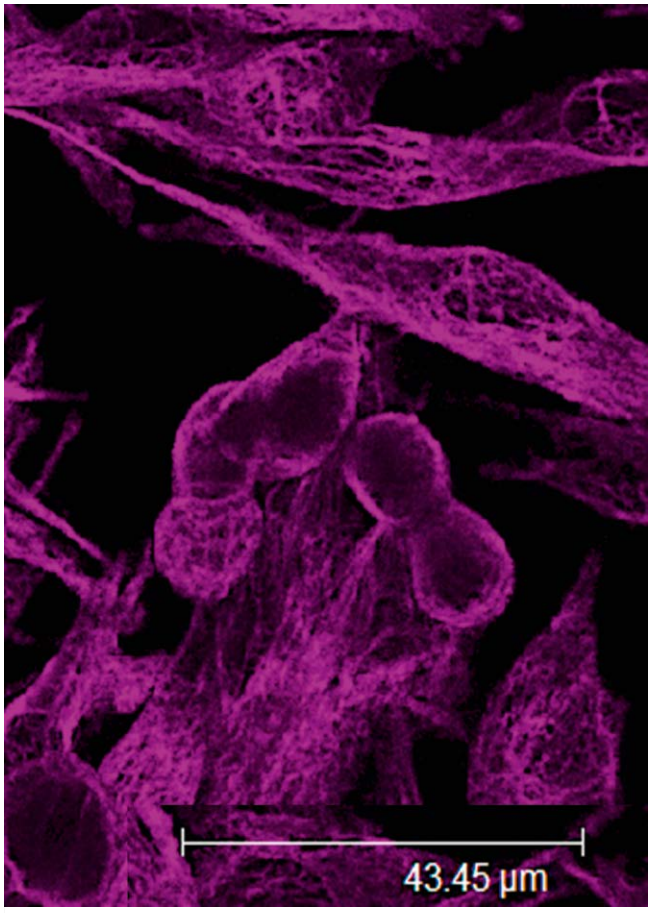

▶ **Fig. 28** LSCM observations of vimentin architecture of M14 WT cells after treatment with 0.01 % TTO for 72 h. At 72 h from the treatment, M14 WT cells recovered the damage induced by TTO and a number of mitotic cells was revealed in the cultures.

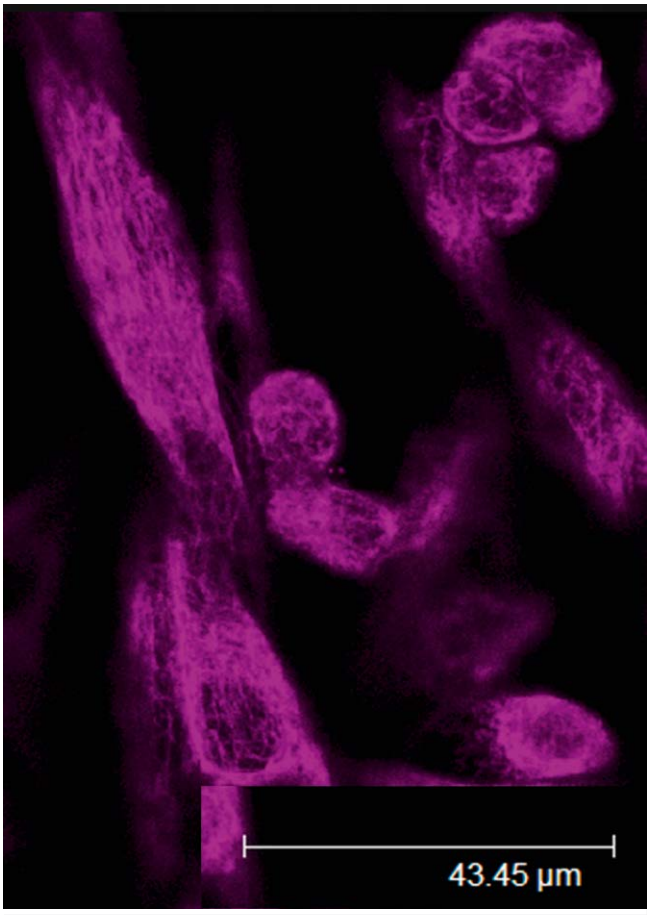

▶ **Fig. 29** LSCM observations of vimentin architecture of M14 WT cells after treatment with 0.005 % terpinen-4-ol for 72 h. M14 WT cells recovered the damage induced by TTO and a number of mitotic cells was revealed in the cultures.

At the end of treatments, for vimentin staining, samples were washed with PBS, fixed for 5 min in methanol (room temperature), followed by 2 min in acetone (− 20 °C), and allowed to air dry for 10–15 min. Then, cells were rehydrated in PBS containing 10 % FBS, 10 % AB serum, and 1 % bovine serum albumin for 10 min and incubated with a mouse monoclonal anti-vimentin antibody diluted 1:50 in the same solution at room temperature. After 30 min, samples were washed in PBS and incubated with a secondary Alexa 633 goat anti-mouse IgG (1:50) for 30 min at room temperature. Cells were then rinsed three times with PBS.

Finally, all samples were mounted in PBS containing 50 % glycerol. Observations were performed using a Leica TCS SP2 LSCM (Leica; Microsystems) equipped with Ar/Kr and He/Ne lasers.

Supporting information

Cell cycle analysis on sensitive and drug-resistant M14 cells after treatment with TTO (0.01 and 0.02 %) and terpinen-4-ol (0.005 and 0.01 %) for 24 and 48 h (**Figs. 1S and 2S**).

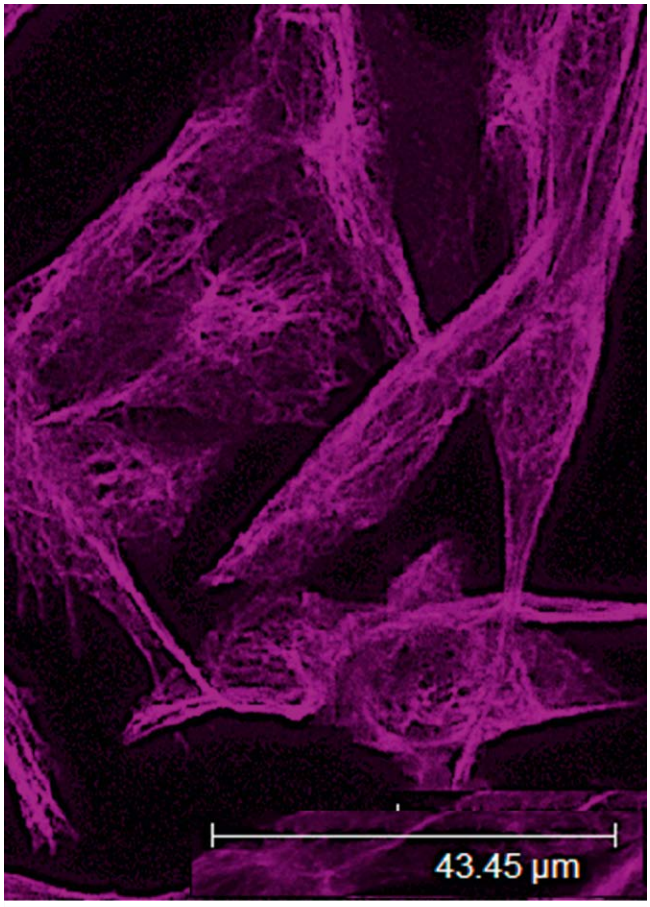

▶ **Fig. 30** LSCM observations of vimentin architecture of untreated M14 ADR cells 72 h from seeding.

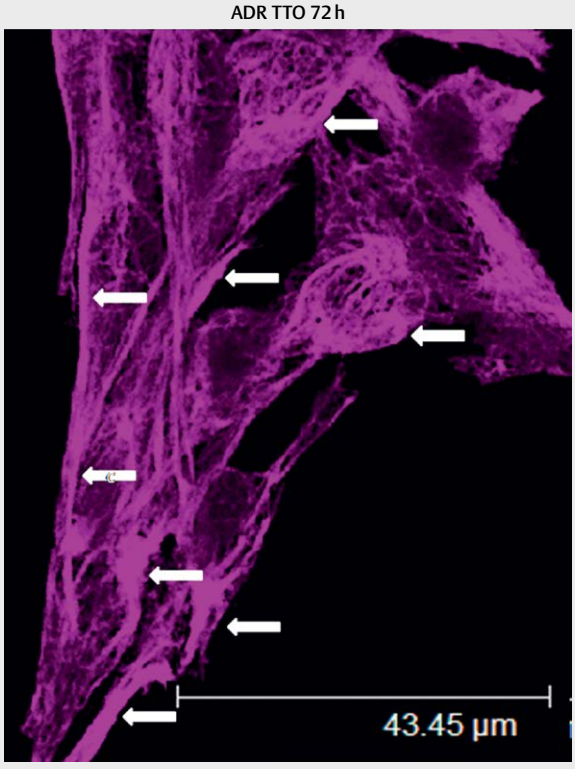

▶ **Fig. 31** LSCM observations of vimentin architecture of M14 ADR cells after treatment with 0.01 % TTO for 72 h. Thick vimentin bundles (arrows) and strongly labeled accumulations (arrows) were still visible in TTO-treated samples.

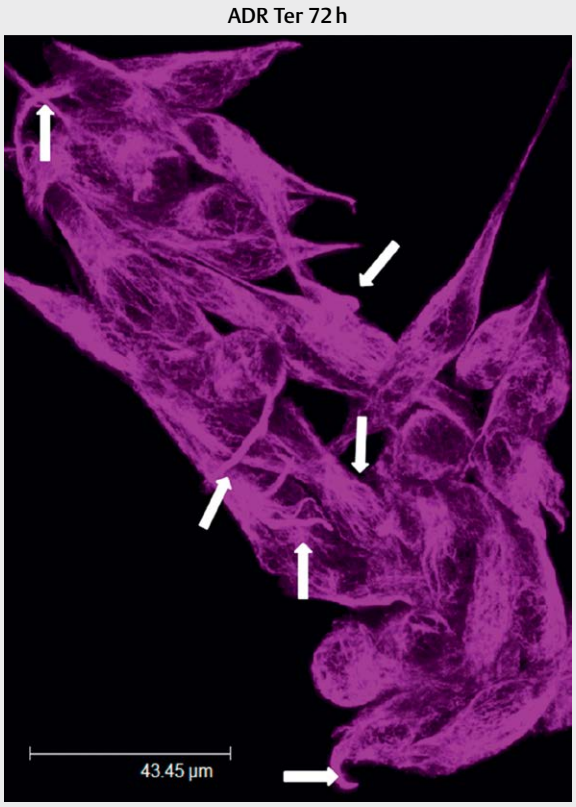

▶ **Fig. 32** LSCM observations of vimentin architecture of M14 ADR cells after treatment with 0.005 % terpinen-4-ol. Distortion and detachment of IF bundles and strongly fluorescent vimentin accumulations (arrows) were detected.

Acknowledgements

We thank Mrs. Laura Toccacieli for her technical assistance.

Conflict of Interest

The authors declare that they have no conflict of interest.

References

[1] Carson CF, Hammer KA, Riley TV. *Melaleuca alternifolia* (Tea Tree) oil: a review of antimicrobial and other medicinal properties. Clin Microbiol Rev 2006; 19: 50–62

[2] Flores FC, De Lima JA, Da Silva CR, Benvegnú D, Ferreira J, Burger ME , Beck RC, Rolim CM, Rocha MI, Da Veiga ML, Da Silva Cde B. Hydrogels containing nanocapsules and nanoemulsions of tea tree oil provide antiedematogenic effect and improved skin wound healing. J Nanosci Nanotechnol 2015; 15: 800–809

[3] Hadaś E, Derda M, Cholewiński M. Evaluation of the effectiveness of tea tree oil in treatment of *Acanthamoeba* infection. Parasitol Res 2017; 116: 997–1001

[4] Labib RM, Ayoub IM, Michel HE, Mehanny M, Kamil V, Hany M , Magdy M, Moataz A, Maged B, Mohamed A. Appraisal on the wound healing potential of *Melaleuca alternifolia* and *Rosmarinus officinalis L*. essential oil-loaded chitosan topical preparations. PLoS One 2019; 14: e0219561

[5] Malhi HK, Tu J, Riley TV, Kumarasinghe SP, Hammer KA. Tea tree oil gel for mild to moderate acne; a 12 week uncontrolled, open-label phase II pilot study. Australas J Dermatol 2017; 58: 205–210

[6] Mazzarello V, Donadu MG, Ferrari M, Piga G, Usai D, Zanetti S , Sotgiu MA. Treatment of acne with a combination of propolis, tea tree oil, and aloe vera compared to erythromycin cream: two double-blind investigations. Clin Pharmacol Adv Appl 2018; 10: 175–181

[7] Messager S, Hammer KA, Carson CF, Riley TV. Effectiveness of hand-cleansing formulations containing tea tree oil assessed *ex vivo* on human skin and *in vivo* with volunteers using European standard EN 1499. J Hosp Infect 2005; 59: 220–228

[8] Rothenberger J, Krauss S, Tschumi C, Rahmanian-Schwarz A, Schaller H- , Held M. The Effect of Polyhexanide, Octenidine Dihydrochloride, and Tea Tree Oil as Topical Antiseptic Agents on *In Vivo* Microcirculation of the Human Skin: A Noninvasive Quantitative Analysis. Wounds 2016; 28: 341–346

[9] Assmann CE, Cadoná FC, Bonadiman BDSR, Dornelles EB, Trevisan G, Cruz IBMD. Tea tree oil presents *in vitro* antitumor activity on breast cancer cells without cytotoxic effects on fibroblasts and on peripheral blood mononuclear cells. Biomed Pharmacother 2018; 103: 1253–1261

[10] Banjerdpongchai R, Khaw-On P. Terpinen-4-ol induces autophagic and apoptotic cell death in human leukemic HL-60 cells. Asian Pac J Cancer Preven 2013; 14: 7537–7542

[11] Calcabrini A, Stringaro A, Toccacieli L, Meschini S, Marra M, Colone M, Salvatore G, Mondello F, Arancia G, Molinari A. Terpinen-4-ol, the main component of *Melaleuca alternifolia* (tea tree) oil inhibits the *in vitro* growth of human melanoma cells. J Invest Dermatol 2004; 122: 349–360

[12] Greay SJ, Ireland DJ, Kissick HT, Levy A, Beilharz MW, Riley TV, Carson CF. Induction of necrosis and cell cycle arrest in murine cancer cell lines by *Melaleuca alternifolia* (tea tree) oil and terpinen-4-ol. Cancer Chemother Pharmacol 2010; 65: 877–888

[13] Khaw-on P, Banjerdpongchai R. Induction of intrinsic and extrinsic apoptosis pathways in the human leukemic MOLT-4 cell line by terpinen-4-ol. Asian Pac J Cancer Preven 2012; 13: 3073–3076

[14] Ramadan MA, Shawkey AE, Rabeh MA, Abdellatif AO. Expression of P53, BAX, and BCL-2 in human malignant melanoma and squamous cell carcinoma cells after tea tree oil treatment *in vitro*. Cytotechnology 2019; 71: 461–473

[15] Greay SJ, Ireland DJ, Kissick HT, Heenan PJ, Carson CF, Riley TV, Beilharz MW. Inhibition of established subcutaneous murine tumour growth with topical *Melaleuca alternifolia* (tea tree) oil. Cancer Chemother Pharmacol 2010; 66: 1095–1102

[16] Ireland DJ, Greay SJ, Hooper CM, Kissick HT, Filion P, Riley TV, Beilharz MW. Topically applied *Melaleuca alternifolia* (tea tree) oil causes direct anti-cancer cytotoxicity in subcutaneous tumour bearing mice. J Dermatol Sci 2012; 67: 120–129

[17] Shapira S, Pleban S, Kazanov D, Tirosh P, Arber N. Terpinen-4-ol: A Novel and Promising Therapeutic Agent for Human Gastrointestinal Cancers. PLoS One 2016; 11: e0156540

[18] Giordani C, Molinari A, Toccacieli L, Calcabrini A, Stringaro A, Chistolini P, Arancia G, Diociaiuti M. Interaction of tea tree oil with model and cellular membranes. J Med Chem 2006; 49: 4581–4588

[19] Colone M, Calcabrini A, Toccacieli L, Bozzuto G, Stringaro A, Gentile M, Cianfriglia M, Ciervo A, Caraglia M, Budillon A, Meo G, Arancia G, Molinari A. The multidrug transporter P-glycoprotein: a mediator of melanoma invasion? J Invest Dermatol 2008; 128: 957–971

[20] Bozzuto G, Colone M, Toccacieli L, Stringaro A, Molinari A. Tea tree oil might combat melanoma. Planta Med 2011; 77: 54–56

[21] Strouhalova K, Přechová M, Gandalovičová A, Brábek J, Gregor M, Rosel D. Vimentin intermediate filaments as potential target for cancer treatment. Cancers 2020; 12: 184

[22] Hall A. The cytoskeleton and cancer. Cancer Metastasis Rev 2009; 28: 5–14

[23] Hohmann T, Dehghani F. The Cytoskeleton-A Complex Interacting Meshwork. Cells 2019; 8: 362

[24] Wen Q, Janmey PA. Polymer physics of the cytoskeleton. Curr Opin Solid State Mater Sci 2011; 15: 177–182

[25] Bershadsky AD, Balaban NQ, Geiger B. Adhesion-dependent cell mechanosensitivity. Annu Rev Cell Dev Biol 2003; 19: 677–695

[26] Geiger B, Bershadsky A, Pankov R, Yamada KM. Transmembrane extracellular matrix-cytoskeleton crosstalk. Nat Rev Mol Cell Biol 2001; 2: 793–805

[27] Hotulainen P, Lappalainen P. Stress fibers are generated by two distinct actin assembly mechanisms in motile cells. J Cell Biol 2006; 173: 383–394

[28] Livne A, Geiger B. The inner workings of stress fibers - from contractile machinery to focal adhesions and back. J Cell Sci 2016; 129: 1293–1304

[29] Gan Z, Ding L, Burckhardt CJ, Lowery J, Zaritsky A, Sitterley K, Mota A, Costigliola N, Starker CG, Voytas DF, Tytell J, Goldman RD, Danuser G. Vimentin Intermediate Filaments Template Microtubule Networks to Enhance Persistence in Cell Polarity and Directed Migration. Cell Syst 2016; 3: 252–263.e8

[30] Seetharaman S, Etienne-Manneville S. Microtubules at focal adhesions - a double-edged sword. J Cell Sci 2019; 132: jcs232843

[31] Tsuruta D, Jones JCR. The vimentin cytoskeleton regulates focal contact size and adhesion of endothelial cells subjected to shear stress. J Cell Sci 2003; 116: 4977–4984

[32] Mellad JA, Warren DT, Shanahan CM. Nesprins LINC the nucleus and cytoskeleton. Curr Opin Cell Biol 2011; 23: 47–54

[33] Ketema M, Sonnenberg A. Nesprin-3: a versatile connector between the nucleus and the cytoskeleton. Biochem Soc Trans 2011; 39: 1719–1724

[34] Starr DA, Fridolfsson HN. Interactions between nuclei and the cytoskeleton are mediated by SUN-KASH nuclear-envelope bridges. Annu Rev Cell Dev Biol 2010; 26: 421–444

[35] Svitkina TM, Verkhovsky AB, Borisy GG. Plectin sidearms mediate interaction of intermediate filaments with microtubules and other components of the cytoskeleton. J Cell Biol 1996; 135: 991–1007

[36] Battaglia RA, Delic S, Herrmann H, Snider NT. Vimentin on the move: new developments in cell migration. F1000Res 2018; 7: F1000 Faculty Rev-1796

[37] Esue O, Carson AA, Tseng Y, Wirtz D. A direct interaction between actin and vimentin filaments mediated by the tail domain of vimentin. J Biol Chem 2006; 281: 30393–30399

[38] Jiu Y, Lehtimäki J, Tojkander S, Cheng F, Jäälinoja H, Liu X, Varjosalo M, Eriksson JE, Lappalainen P. Bidirectional interplay between vimentin intermediate filaments and contractile actin stress fibers. Cell Rep 2015; 11: 1511–1518

[39] Sakamoto Y, Boëda B, Etienne-Manneville S. APC binds intermediate filaments and is required for their reorganization during cell migration. J Cell Biol 2013; 200: 249–458